A Reproduced Copy

OF

The George W. Woodruff
School of Mechanical Engineering

Georgia Institute of Technology

Atlanta, Georgia 30332

GEORGIA TECH 1885-1985

DESIGNING TOMORROW TODAY

THE GEORGE W. WOODRUFF SCHOOL OF
MECHANICAL ENGINEERING

M.E. 4182
MECHANICAL DESIGN ENGINEERING

NASA / UNIVERSITY
ADVANCED MISSIONS SPACE DESIGN PROGRAM

SKITTER FOOT DESIGN

AUGUST 25, 1987

Gene Choi
David L. Jones
James Morris
Martin Parham
Jim Stephens
Gregg Yancey

Georgia Institute of Technology
Atlanta, Georgia 30332-0405

ABSTRACT

A mechanical design team was formed to design a foot for the lunar utility vehicle SKITTER. The primary design was constrained to be a ski pole design compatible with the existing femur-tibia design legs.

The lunar environment had several important effects on the foot design. Investigation of the lunar soil revealed that the density and grain size of the soil varies considerably, causing large variations in the bearing capacity of the soil. The temperature range of the lunar surface, (-187 to +102 degrees C), was a primary factor in the material selection. Gravity on the lunar surface was determined to be one-sixth of the earths gravity, or 1.62 meters per second squared.

Three materials were investigated for the SKITTER foot; aluminum alloys, cold worked stainless steel alloys, and titanium alloys. Aluminum alloys have a high strength to weight ratio, but are not very temperature resistant. Aluminum alloys are also susceptible to abrasive wear, due to low hardness. Stainless steels were considered due to their high strength and toughness. The disadvantage of stainless steels is their high weight, especially as compared to titanium alloys. Titanium alloys have good strength to weight ratios, and retain their high strength at extreme temperatures. The titanium alloy selected, Ti-6Al-4V, has high strength properties at high and low temperatures, and is very tough.

Thin film coatings were investigated as a method of wear reduction for the foot. Though the coatings investigated have excellant wear properties, current coatings do not guarantee completely intangible wear. However, coatings do offer reduced wear. At this time, hardfacing appears to be the best possibility for an effective coating.

The performance of the foot is dependant on the action of the legs. The range of motion for the legs was determined to be vertical to 15 degrees above horizontal. The loading on the foot during different operations is unknown, so the maximum loading was assumed to be in the crane position. The crane load produces 27 kN shear and 16.8 kN compression in the foot. An impact analysis was performed for the foot movement, but the results were determined to be inconclusive due to unknown soil parameters.

The initial foot design configuration consisted of an annulus attached to pointed pole. The annulus was designed to prevent excess sinkage. Later designs call for a conical shaped foot with a disk at the point of tibia attachment. The conical area is designed for a sinkage of 20 cm. under average soil conditions for crane loading. The sinkage for normal operation should be less than 20 cm. The conical foot design represents 6.2% of the total SKITTER weight. Also, the conical design allows substantial volume for the insertion of the tibia members into the foot for attachment.

The conical design was analyzed for strength and deflection by two different approaches. A deformable body analysis was performed for the foot under crane load in crane position, and also under actuator load in the vertical position. In both cases, the deflection of the foot was insignificant and the stresses well below the strength of the titanium alloy.

TABLE OF CONTENTS

INTRODUCTION

On June 23, a mechanical design team was formed to design a foot for the three-legged lunar utility vehicle, SKITTER (spatial kinematic inertial translatory tripod extremity robot). The SKITTER is a prototype multiple-use vehicle that will be used in the construction of a manned space station on the moon.

The SKITTER foot design has been prepared as a requirement for the Senior Mechanical Design course, M. E. 4182. The design team consists of six senior mechanical engineering students, under the direction of Dr. Wendell Williams.

The foot design team was instructed to design a prototype foot, based on the current SKITTER design and purpose. Assumptions were to be made for several design parameters due to the fact that the SKITTER design is currently incomplete. Later generations of design may require modifications to the prototype foot design.

The first step in the foot investigation was to determine the design requirements for the foot. These requirements were divided into three general areas: environment, material selection, and loading characteristics. After the requirements were determined, the team investigated different possible shapes for the foot, as well as the material possibilities. Along with the materials investigation, the team considered possible coatings for the foot, to increase the wear resistance.

PROBLEM STATEMENT

The lunar utility vehicle, "SKITTER", is in need of a foot apparatus to attach to the three femur-tibia design legs. The foot design should be compatible with the lunar environment requirements, including temperature variation constraints, gravitational effects, dust contamination, and soil weight support characteristics. While the SKITTER is in the walking mode, the foot should grip the surface in order to prevent slippage after the it is placed down. However, the foot should also release easily when the it is lifted. Weight should be kept low to minimize inertia loss in the foot during movement of the SKITTER. All terrain capability is also required for the foot.

The primary foot design is constrained to be of a ski pole design, with a circular ring to prevent slippage and a pole to allow gripping of the surface. Alternate designs may also be submitted with the ski pole configuration.

A prototype foot could be constructed and placed on the existing scale model SKITTER. If and when the soil experiment group determines a method to approximate lunar soil conditions on earth, the prototype foot could be tested for gripping and release, support ability, and range of motion performance.

LUNAR ENVIRONMENT

The lunar environment is a critical variable in the design of the SKITTER foot. The SKITTER foot must be able to perform in the harsh conditions of the lunar environment. There are five major areas of concern in the lunar environment. These are soil characteristics, temperature variation of the lunar surface, gravity, dust and sinkage of lunar surface.

SOIL CHARACTERISTICS

Lunar soil is produced primarily by meteorite impacts on the lunar surface; the usual terrestrial agents of soil formation are absent on the moon. The soil consists of complex mixtures of mineral fragments, miscellaneous glasses, agglutinates, and lithic fragments. Although the proportions of the various particles types vary, the grain size distributions for the soil falls within a relatively narrow band. The grains are classified as well-graded silty sands. The average particle size usually varies from 0.04 to 0.13 millimeters.

The lunar surface is composed of granular material with a wide size range; coarse blocks of rock and smaller fragments are set in a matrix of fine particles too small to be resolved. Angular fragments occupy approximately 0.8 % of the surface area and have a volumetric median grain size of

130 mm. The volumetric grain size of all fragment material on the surface is much smaller, probably 1 mm or less. The specific gravity of lunar soil samples varies from 2.90 to 3.24 and individual particles range from 1.0 to over 3.32. The bulk densities vary from 0.87 to 1.89 g/cm^3. The ranges in the densities are due to the differences in the porosity, particle shape, surface texture, and grain arrangements.

DATA

Properties of lunar soil

(NASA report - the Apollo and Surveyor Projects)(6)

Bulk Density	1.5 to 2.0 g/cm^3 depending on method of placement and stress history. (Estimate range of 1.55 to 1.65 g/cm^3 for the average density of top 40 cm)
Angle of internal friction	30 degree @ low density to 46 degree @ high density in triaxial compression.
Cohesion	0.01 to 0.15 psi depending on density and moisture content.
Permeability	0.0007 cm/sec @ Density = 1.8 g/cm^3 0.0021 cm/sec @ Density = 1.5 g/cm^3
Dynamic bearing resistance	4 x 10^5 to 7 x 10^5 dynes/cm^2 @ touch down velocity of 3.6 m/s.
Static bearing capacity	2 x 10^5 to 6 x 10^5 dynes/cm^2.

TEMPERATURE VARIATION

The sole source of the moon's heat is derived from its illumination by the sun. Its mean temperature would be

essentially equal to that of the earth were it not for the lack of atmosphere. Its extremes are very different. Based on the observations at Apollo 15 and 17 sites, the temperature varies approximately from +102 C to -187 C. Due to the insulating properties of lunar surface material, the effects of the daily heat or cold wave do not penetrate deeper than about 50 cm. Thermal radiation from these depths remains constant day and night and corresponds to a mean temperature about -30 C.

Data

Long term temperature observations at Apollo 15 and 17 sites

Apollo 15 site	1972 to 1974				
Max. daily temperature range	+ 77	C	to	+ 93	C
Presunrise temperature range	-196	C	to	-184	C
Apollo 17 site	1973 to 1974				
Max. daily temperature range	+ 95	C	to	+102	C
Presunrise temperature range	-187	C	to	-185	C

LUNAR GRAVITY

The force of gravity on the moon's surface is one sixth that of the earth. Gravity is weaker on the moon because the moon's mass is about 81 times smaller than the earth's mass. Lunar gravity is approximately 1.62 m/sec 2

LUNAR DUST

According to the Apollo projects and the Surveyor projects, the dust on the surface of the moon is very abrasive and microscopic. Due to the vacuum and electrostatic forces, it also tends to "stick" to any available surface. The low gravity allows it to the travel vary far when stirred up. The Apollo astronauts discovered the importance of controlling this dust when a fender on the lunar rover broke. Severe dust contamination caused rapid failure of the bearings. Because it is highly abrasive, all moving parts must be sealed from this dust. The dust contains a substantial number of spheres and angular particles that range in size from a fraction of a micron to approximately 4 micrometers.

SINKAGE OF LUNAR SURFACE

The lunar surface is covered with a fine-grained soil whose depth varies from 1 cm to at least 15 cm. To a depth of several millimeters, the soil appears less dense, softer, and more compressible than underlying material (density of single rock was in the range 2.4 to 3.1 g/cm^3). The sinkage data and the peretration resistance of the lunar surface had been collected from the depth of footpad sinkage (6) and the penetration tests of the Apollo Project (see App. 7-1).

Data

Sinkage data from the Surveyor Project

Surveyor	I	III	V	VI	VII
Mass (kg)	295	306	304	300	306
Depth of foot pad sinkage (cm)	3	2	3	4	4

* The foot pad diameter is 30.5 cm at top and 20.3 cm at bottom.
* The surveyor has three foot pads.

MATERIAL SELECTION

In order to achieve a state-of-the-art design for the SKITTER's foot, we examined titanium alloys, aluminum alloys, and cold worked stainless steels as possible choices for the material. The criteria for selection were high strength characteristics, extreme temperature properties, low weight, high toughness and good formability. With special emphasis on the former three qualities, we selected Ti-6Al-4 (solution treated and aged) as the material for the foot.

ALUMINUM ALLOYS

We began investigating aluminum alloys because of their excellent strength-to-weight ratios. Alclad 2219 has a density of 2.85 Mg/m^3 but has a relatively low tensile strength. This material is often used in applications were weight plays a significant factor such as in supersonic aircraft skin and structure components. For applications over a temperature range of -269 to 300 C, aluminum alloys exhibit high fracture toughness. We ruled Alclad 2219 out because of low tensile strength, performance at elevated temperatures, and low hardness which leads to poor wear resistance.

STAINLESS STEELS

In considering stainless steels, we examined the properties of austenitic 304 in the cold worked condition. It possesses excellent ductility, formability, and corrosion resistance. Cold working brings the austenitic to strengths higher than ferritic stainless steels and makes it a good choice for high strength applications. The METALSELECTOR software program, published by the American Society of Metals, retrieved two stainless steels from its' data base when a sort for materials possessing high strength, heat resistance, and fatigue resistance was performed. The software had no parameter for the inclusion of weight when performing a sort. The density of stainless steel (8.03 Mg/m^3) is high relative to similar strength alloys and makes it an unattractive choice in terms of cost.

TITANIUM ALLOYS

Titanium alloys are one of the few non-ferrous alloys that obtain high strength levels. They can develop strengths near 115 kpsi and the strongest tops out at around 180 kpsi. We compared and contrasted two titanium alloys: Ti-6Al-4V and Ti-10V-2Fe-3Al (See Fig. 4.1). Ti-6Al-4V is used in applications where high strength is required in temperatures up to 600 F (See App. 4-1).

Table 4.1 Properties of Titanium Alloys at 200 C

Material	0.2% Yield Strength (MPa)	Tensile Strength (MPa)
Ti-6Al-4V STA	850	960
Ti-10V-2Fe-3Al STOA	710	820

When titanium is subjected to a constant load at an elevated temperature, it will experience creep and undergo a time dependent increase in length. Figure 4.2 in the appendix gives creep rupture data for Ti-6Al-4V and Ti-10V-2-FE-3Al (See App. 4-3 for fatigue data).

The effects of subzero temperatures must also be considered in selection of materials for lunar applications. The material needs to retain high levels of fracture toughness at all temperatures in order to avoid failure in use. In general, yield strengths and tensile strengths of structural alloys increase as the exposure temperature is decreased. Many of the available titanium alloys have been evaluated at subzero temperatures but service at such temperatures has been gained only for Ti-6Al-4V and Ti-5Al-2.5Sn. Tensile and yield strengths are shown in appendix

4-3, fatigue life tests and fatigue crack growth rates in App. 4-4, fracture toughness in App. 4-5, and Young's modulus and Poisson's ratios in App. 4-5. These alloys have very high strength-to-weight ratios at cryogenic temperatures and have been the preferred alloys for special applications from -320 F to -452 F.

Ti-6Al-4V (STA) was chosen primarily because of its density (4.43 Mg/m^3) and high strength properties (See table 4.2, below). The density of titanium is about 60% that of steel making it advantageous over high strength steels in space applications. Ti-6Al-4V can be hot or cold formed, has excellent corrosion resistance, and can be machined and welded.

Table 4.2 Properties of Materials at 25 C

Material	Density (Mg/m^3)	Tensile (GPa)	Yield (GPa)	% Elong
Ti-6-4	4.43	1.0343	.9653	8
Alclad 2219	2.85	.3999	.2758	12
Austenitic 304	8.03	1.2756	.9653	9

HARD COATING APPLICATIONS

INTRODUCTION TO MAGNETRON SPUTTERING

Wear is a tribological problem that has existed since the dawn of time. Various methods have been used to reduce it to lower levels. Previous techniques required thick, heavy coatings to be bonded to base materials. Recent technology, however, has allowed for the creation of thin films. These new films offer excellent hardness and wear resistance. Chemical Vapor Deposition, Ion, and Magnetron sputtering are among several different coating processes available. The magnetron sputtering process has been chosen as the most feasible technique for use in lunar applications due to its high bonding strength.

SPUTTERING TECHNIQUE

A magnetron sputtering device, consists of two major components, a sputtering head and a magnet assembly. Complimentary pieces of the system include a vacuum chamber, heating unit, and cooling system. The procedure requires an inert gas like Argon, and a gaseous reagent such as Nitrogen. Because different systems operate at distinct pressures, temperatures, and use various reagents, only a general process description is provided.

The magnetron sputtering process produces a hard or soft coat film on a substrate by the reaction of a sputtered element such as Titanium in an controlled atmosphere of a reagent like Nitrogen or Carbon. The first step of the procedure is to insert the specimen and evacuate the chamber. Next the substrate is heated to about 200 degrees Celsius and the chamber is backfilled with Argon gas. When this is completed, a charge is induced across the cathode and anode parts of the sputtering head and a plasma is formed. Following plasma ignition, the power is increased and the pressure is lowered until a optimal operating condition is reached and the coating begins to form on the substrate.

The magnetic sputtering technique was chosen because of its high bonding strengths at relatively low bonding temperatures. For example, the Chemical Vapor Deposition (CVD) technique requires temperatures in the 500 to 1400 degree Celsius region, creating possible problems with the titanium alloy substrate. The Ion coating technique, does not produce a hard film with sufficient bonding strength. The magnetron sputtering technique is the sole thin film coating process that is potentially suitable for lunar applications where high temperature gradients and a hard vacuum exist.

AVAILABLE MATERIALS

There are many suitable materials available for the hard coating of a substrate. Titanium, Magnesium, and Tungsten are among the metals available for sputtering. Nitrogen, gaseous Carbon, and gaseous Boron are suitable for reagents. Appendix includes some possible combinations of sputtered metals and reagents.

WEAR CHARACTERISTICS

Two parameters greatly influence the service life of hard coated components in the lunar environment. These are abrasion and film thickness. Because of the moon's soil characteristics, abrasion dominates all of the wear mechanisms in the SKITTER foot design.

ABRASION CONTROL

One major parameter that affects the abrasion resistance of any material is the hardness. If Ha is defined as the hardness of the abrading material and Hm as the hardness of the material being abraded, then we define the hardness ratio as Ha/Hm. For negligible wear, a hardness ratio of .2 to .6 is desired. In a lunar application, this is not possible since silicon, which is a principal ingredient in lunar soil has a Vickers hardness of around 3500 and the hardest thin

films available have Vickers hardnesses in the 2500 to 3200 range (See App. 5-1). Unfortunately, according to Krushchov's data (16), we are in the light wear range where Ha / Hm is between 0.72 to 1.12. Thus a ski pole foot, as in our project, would experience small but tangible wear regardless of which currently available hard coatings is chosen.

The abrasive wear resistance of thin films is conditional on the development of improved coatings. At present, thin films are categorized into two types, simple and complex. The simple coatings involve only one base element such as titanium while the complex coatings may involve several elements like Chromium, Tungsten, and Vanadium. Recent developments have led to speculation that increased hardnesses may be obtained with the complex coatings (18). As of this date, only a meager amount of information is available on the complex coatings. Also, abrasive wear tests for films abraded by silicon have not ever been completed. However, it is anticipated that the complex thin films will offer potential for controlling abrasive wear.

FILM THICKNESS

To bond properly to the substrate, a magnetron sputtered film needs to be very thin, optimally in the three to ten micrometer range. This creates a dilemma when dealing

with the abrasion characteristics of lunar soil. Even though we have identified contemporary hard coat technology as confining abrasive wear to the light wear region, measured wear will still exist. A thin film will be worn away in a relatively short period of time when Si, the primary ingredient of the moon's soil, is the abrading material. The solution to this is the development of better coatings.

To determine the precise thickness of a thin film, one must identify the wear rate of the material. The wear rate is equal to an empirical constant times the load divided by the bulk hardness of the abraded material. One can see that an increase in hardness or a decrease in load will reduce the wear rate. In a thin film, however, only a minute wear rate is tolerable if the component is to be designed for a long service life. Therefore, unless the wear rate of the SKITTER foot design is infinitesimally small, the hard coat will be worn away and deterioration of the foot will ensue.

COEFFICIENT OF FRICTION VS. FILM THICKNESS

In examining the relationship between the friction coefficient of the hard coated substrate versus the thickness of the applied hard coat, it is noted that "under the heavy load the coating thickness has no effect on the friction coefficient, except that the friction coefficient tends to be lower for the minimum film thickness." (15). Under lighter loads, the steady state friction coefficient varies with the

applied coating thickness. Unfortunately, there is not sufficient experimental verification to prove whether the frictional characteristics of hard coated specimens are dominated by the properties of the hard coat or the mechanical properties of the underlying substrate. It is therefore difficult to identify a theoretical relationship between film thickness and the coefficient of friction. The only guide to estimating the friction coefficient at various film thicknesses is to compile empirical data for the desired film thickness. The main premise is as stated above; under light loads, the friction coefficient varies with film thickness and under heavy load the coating thickness has no effect on the coefficient of friction except for the minimum film thickness.

Future abrasion control processes will involve the reduction of friction between the lunar soil and the foot for SKITTER. Contrary to conventional thought, the reduced wear characteristics of hard coated materials is not due to a decrease in friction. In fact, the friction coefficient is larger between hard coats and an abrading material than it is between uncoated materials and the same abrading surface (15). Careful modification of the surface structure of the hard coatings should decrease friction. Among these modifications include the removal of all sharp edges and surface defects of the hard compound. Reduction of friction could eventually lead to an additional decrease in wear of the SKITTER foot.

BOND STRENGTH OF HARD COATS

In a thin film, a high bond strength is necessary to prevent delamination. The main parameter of material compatibility for the coating and the substrate is the product of the Young's Modulus of elasticity and the coefficient of thermal expansion (17). The substrate should have a E times alpha product within plus or minus twenty five percent that of the hard coating. The thickness of the film is also important to the bond strength of the coating. For example, a film that is too thick can be subject to stresses caused by thermal gradients across the material interface. In addition, excessive film thickness can lead to spalling in certain types of loading (19). It is important to note that film failure could lead to additional delamination and thus the eventual wearing of the substrate.

CURRENT ALTERNATIVES TO THIN FILMS

Hardfacing

Hardfacing is one available technique for wear reduction due to abrasion. Hardfacing applies a relatively thick, hard material, usually one centimeter or more, onto a softer base material. Used primarily in the ore processing and earth moving equipment, hard facing is in use today with a high

success rate. The major drawback for lunar applications is the high thermal gradient.

Hardfacing bond strength is a function of the coefficient of thermal expansion of both the base material and the mating material. The high thermal gradients present on the moon will subject the interface between the materials to high thermal stresses. This could cause the facing to debond from the material.

Naturally, there are ways to provide increased wear protection with hardfacing. To establish the areas of the SKITTER foot which would need the most hardfacing, the wear patterns must be considered. This would require an experiment which would simulate the wear patterns of the foot. When completed the results would be compiled and more hardfacing would be applied in the areas with maximum wear.

Low Stress Loading

Low stress loading is a another way to reduce abrasive wear. This was demonstrated earlier when the wear rate was defined as being proportional to the load. Since the loads on the SKITTER have already been determined, the best method to reduce the stress per unit area on the foot is to increase its contacting surface area. Unfortunately, to obtain sufficient surface area, this would call for a relatively flat or hemispherical foot with no central spike, thus violating the ski pole design constraint.

CONCLUSIONS ABOUT WEAR REDUCTION

In their present state, thin films are not suitable for use on the foot for SKITTER. Though they bond well with many base materials and have good thermal properties, they are not currently capable of surviving abrasion dominated wear regimes when silicon is the abrading material. Research should be initiated immediately to search for a technique to reduce the effects of abrasive wear on thin films. Until resistance against silicon abrasion is dramatically increased, thin films should not be used and alternatives such as hardfacing should be considered.

Hardfacing is a proven technique of controlling abrasion. However, the large thermal gradients at the interface between the base material and the hardface could be a problem at both the high and low temperature extremes in the lunar environment. Testing at the lunar temperature extremes must be completed before hardfacing can be used. Otherwise, it seems to be the most reliable method for abrasion resistance available at this time.

Low stress loading can reduce abrasive wear by an increasing the surface area, thus, decreasing force per square inch of the foot. This method does not conform to the ski-pole constraint. Also, additional weight is accrued by the increasing of the surface area. This technique to reduce abrasive wear is not recommended.

FORCE ANALYSIS

RANGE OF MOTION

To fully examine the various forces and stresses on the foot of the skitter, one must first analyze the different positions in which the skitter will perform its functions.

Although details of skitter's walking motion are still unknown, a general concept of its movement has been assumed. The skitter leg/actuator design has been planned to provide a leg sweep angle of approximately 125 degrees (See App. 6-1). Since each actuator can assume any length between its minimum and maximum lengths, the foot can reach any point within the given range of motion shown on the graph, giving the skitter the ability to traverse rugged and inconsistent terrain (8). As a result, the leg design enables each foot to reach a maximum position of 75 degrees relative to vertical position (i.e., 15 degrees above horizontal) (8).

DIVERSE LOADING

The variety of operations performed by the SKITTER produces a number of different loading configurations on the foot. In the crane position, the foot assumes a position of approximately 58 degrees above horizontal. In this configuration, the foot sustains a vertical force from the lunar surface, producing a shear force (V) and a compressive

force (P). When drilling, a force perpendicular to the planes of the shear and compressive forces would also be assumed as seen in App. 6-2. Soil bagging and digging operations will involve similar combinations of forces. The maximum force exerted on the foot in its four operational configurations is assumed to be sustained during the crane operation, when the foot will be subjected to maximum forces of 27 kN in shear and 16.8 kN in compression (8).

IMPACT ANALYSIS

The first force on the foot considered is that of impact occurring during normal maneuvering of the SKITTER. The force in this analysis results from the load sustained during the walking operation. When walking the SKITTER transfers its center of mass forward while extending its lead leg. The vehicle then falls forward onto the lead foot. Actuator lengths in the legs are then changed to keep the vehicle's center of mass moving forward so that the rear legs can be brought forward. At this point, the SKITTER continues forward, extends its front leg, and the process is repeated (See Fig. 1).

The following analysis examines impact force exerted on the foot when entering the soil. This force occurs through a change in momentum over the period of time in which the foot enters the soil, making it an impulse force. Furthermore, it is assumed that the greatest impact force will be sustained

by the front foot, since it will withstand a large portion of the vehicle's weight under free fall conditions.

To obtain a value for this impulse force, the acceleration term must be replaced by a value reflecting the change in velocity over the period of time in which the foot sinks into the lunar soil. When multiplied by the SKITTER's mass, this value represents the change in momentum of the SKITTER (as it decelerates through the soil) divided by the length of time between the foot's entrance into the soil and the point at which the foot comes to a complete stop (10). In reality, the actual impulse force might be closer to one third of this value, since three feet support the mass of the SKITTER. However, this calculation represents a worst-case scenario (See App. 6-3).

To determine the length of time taken for a particle with a given entrance velocity to completely stop in the lunar soil, the soil's damping characteristics must be known. Since damping information on the soil could not be obtained, the calculated change in momentum has been divided by a series of t-t(0) values in increments of 0.005 seconds. Under the given calculations, a foot supporting the entire mass of the SKITTER would have an impact force corresponding to the t-t(0) value taken for the foot to complete its penetration through the soil (See App. 6-4). Although this operation represents a relatively large force on the foot, it must again be noted that damping characteristics of the lunar soil are unknown, preventing calculation of penetration time

for given masses and foot designs. It is also inherent that normal walking operations would involve a much smaller change in the height of the SKITTER's center of mass, and that only a fraction of the SKITTER's total mass would be supported by the front foot. For example, assuming a 1.5 m change in height of the SKITTER and the foot's support of one third of the mass, the change in momentum would be only 15.1% of the maximum value calculated (See App. 6-3A). As a result, the lack of knowledge of lunar soil and the SKITTER's walking characteristics prevent use of forces calculated from this analysis to be used in a deformable body analysis.

FOOT CONFIGURATION

ANNULUS DESIGN

As mentioned in the problem statement, the primary foot design is constrained to be a ski pole type design. The ski pole design was envisioned to be an annulus attached to a titanium block at the end of the tibia, with a narrow point below the ring (see fig. 5). The point would provide traction during the walking motion, while the annulus would provide the surface area necessary to prevent sinkage.

Investigation into the SKITTER leg motion revealed that the foot must operate at a wide range of angles to the surface. As the angle between the tibia and the surface decreases, the annulus would come into contact with the surface. This condition could generate a tremendous bending moment in the annulus, since it would support the vertical load. To support the load, braces were added between the annulus and the tibia members (See Fig.6).

Preliminary soil investigations revealed that the surface area of the annulus would have to be increased to prevent sinkage. The surface area was increased by changing the annulus from a tubular ring to a flat disk (See Figure 7). The edge of the disk was beveled to provide better support at low angles. Also, the point of the foot was changed to a conical shape.

The conical shape greatly reduces the stress at the top of the point, by increasing the stressed area. As the tibia angle decreases, the top of the point must accept increasing shear forces due to the moment about the tip. The use of the conical shape reduces the stress concentration.

CONICAL DESIGN

The concept of a conical point produced a new design idea. Instead of relying upon the annulus to resist penetration of the lunar soil, a conical point could be used to resist sinkage (See Figure 8).

The conical foot design has several advantages over the annulus design. The purpose of the conical foot design is to use the cross-sectional area of the cone to resist sinkage. Although the annulus is no longer required to resist sinkage, it still performs a needed function for the foot. The disk provides an envelope for the attachment of the tibia members to the foot, as well as providing additional surface area in case of extreme sinkage.

Sinkage Analysis

In order to dimension the conical foot design, a sinkage analysis was performed. The length of the foot is determined by the constraint that the leg length remain as designed.

Therefore, only three dimensions remained to be determined: the cone angle, disk diameter, and the disk height.

The most important factor in determining the cone angle is the sinkage parameter. Since the density and compressibility of the lunar soil varies considerably, an acceptable sinkage level under average soil conditions was selected. For design purposes, it has been decided that an average sinkage of 20 cm during the maximum load would be acceptable. The maximum load (31.7 kN) occurs in the crane position at an angle of 51.56 degrees (See fig. 4).

To determine the penetration resistance of the lunar soil, data collected from the soil experiments of the Lunokhod 1, Apollo 14, 15, and 16 missions was used (See App. 7-1). The data is based on penetrometer tests performed using a conical penetration device . The graph in Appendix 7-1 illustrates the broad range of sinkage resistance from different sites.

In order to determine an appropriate cone angle, the maximum and minimum penetration resistance was determined for eight different sinkage levels (See App. 7-2). With a known load (crane load) being considered, the maximum and minimum cone area requirements were calculated. Since the penetrometer tests were conducted in the vertical position, the crane load was considered to be vertical. The required cone area was considered to be the cross-sectional area of the cone along the surface for a given penetration. From the calculation of the area, the cone angle was determined by

geometry. Using the design parameter of average penetration resistance at a sinkage level of 20 cm, the required cone angle was found to be 36.92 degrees (See Fig. 9).

The approximation of a vertical crane load was a rather conservative approach which yielded a large cone angle. If the foot is considered to be in the crane position, the cross-sectional area at the surface would be elliptical instead of circular. Correction of the calculations for the elliptical area resulted in a cone angle of 23.76 degrees for average penetration resistance at 20 cm sinkage (See App. 7-3). At that cone angle, the foot is a streamlined, compact unit (See Figure 10). The cone angle is slightly greater than the angle between the tibia members, allowing adequate support for attachment to the tibia members. The disk and upper pocket provide ample distance (21 cm) for bonding to the tibia members, as well as providing multi-directional support.

Weight Analysis

Initial weight calculations for the foot shown in Figure 10 resulted in a weight of 214.7 kg per foot (See App. 7-4 for calculations). Using an estimated weight of 5454 kg (12,000 lb), the three feet would contain 10.6% of the SKITTER weight. In order to minimize actuator weight and size, an effort was made to reduce the weight of the foot. A target foot weight of 4-6% total SKITTER weight was set to

prevent actuator oversizing. To achieve the necessary weight reduction, the disk was moved down the cone 10 cm (See Figure 11). The envelope depth for the tibia members was increased from 21 to 25 cm, although the diameter of the tibia members would have to decrease inside the foot. The reduced weight design lowers the foot weight to 6.2% of SKITTER weight (See App. 7-5 for calculations).

Overall, the conical foot design illustrated in Figure 11 satisfies all of the design requirements. The foot should provide adequate traction while walking yet release easily when lifted. The design allows the height of the SKITTER to remain the same as designed, while providing substantial support for the attachment of the tibia members.

Attachment to the Tibia Members

The existing leg design calls for a titanium block to receive the tibia members and attach the foot. The tibia members would be bolted into holes in the block. This method of attachment could be used with the conical foot, using the upper foot as the bolting block.

The existing leg design uses circular struts constructed of a woven boron/epoxy composite with a honeycomb core. It has been mentioned that the leg design may change, due to the shear and bending forces generated in the circular cross-section. If the design and/or material of the struts were to change, the conical foot would provide an excellent envelope

for strut attachment. If the material of the members were changed to an alloy, bonding of the members to the foot could be considered as an alternative to bolting. Whatever method is used, the members should be inserted into the foot to insure adequate support.

DESIGN ANALYSIS

DEFORMABLE BODY ANALYSIS

Since the 31.7 kN load from the crane operation is assumed to be the maximum force exerted on the foot under normal conditions, an analysis of normal, shear, and bending stresses incident on the foot has been provided for this operation.

The 31.7 kN force, incident at an angle of 32 degrees relative to the centerline of the foot, is broken into its components of 16.8 kN in compression (P) and 27.0 kN in shear (V) (See App. 8-1). Using the given foot configuration, radii from the centerline to the outer shell of the foot are dimensioned according to their respective lengths. From these dimensions, differential areas and moments of inertia are computed at each length along the foot. With these values, Mc/I, P/A, and V/A stresses are obtained for each point along the foot, as shown in App. 8-2 (10). The values of shear force (V), length along the foot, Modulus of Elasticity (E), and Moment of Inertia (I) are also used to compute the differential deflection at each length (See App 8-3). Finally, differential lengths between points of measurement are used with normal force (P), E, and the cross-sectional area (A) to compute the differential change in foot length (delta). The sum of these differential changes in length reflects the overall change in length of

the foot under this maximum crane load (10).

Bending stress changes with the distance from the foot's neutral axis. Therefore, maximum bending stresses are obtained by calculating Mc/I with c equal to the cross-sectional area radius, since the radius represents the limiting value of c. The upward direction of the force produces a compressive bending stress on the top surface of the foot and a corresponding tensional stress on the foot's bottom surface. These values are added to the compressive P/A value to obtain normal stress values along the top and bottom surfaces of the foot (See App. 8-4).

From the results listed in Figure 8-3, maximum bending stress is found to be +/- 21.9 MPa at the top section of the base of the foot, where the foot and tibia members meet; maximum normal stress, -7.3 MPa at the tip of the foot; and maximum shear stress, -11.7 MPa, also at the tip. The maximum stress in tension of 21.3 MPa falls well under the yield strength of Titanium, 1102.4 MPa (@ room temperature). Similarly, the change of overall height of the foot under this load is 0.0000045 m, an insignificant value. In computing cantilever deflection, the equation for cantilever-end load deflection equation (1) must be modified due to the changing moment of inertia along the length of the foot. This problem is solved by considering a differential length of the foot to be located at the wall, computing the deflection of the differential length at its distance from the load, and summing the deflections of each differential

length along the foot. Using this technique, no measurable deflection was recorded. Graphical analysis of these results are provided in Apps. 8-5,6.

CANTILEVER ANALYSIS

An analysis similar to that performed for the crane operation involves using the maximum actuator output to impart the largest possible horizontal force on the foot when located in a vertical position. Performance of this test reflects the difficulties that might be encountered if the front foot were to be stopped at the tip by an immovable object while moving forward across the lunar surface. By considering the tibia as a beam with its connection to the femur fixed, the opposing moment exerted by an immovable object at the tip of the foot produces a 46.1 kN force, perpendicular to the vertical direction of the foot (See App. 8-7). Stress calculations were determined in exactly the same manner as those from the crane operation, the only exception being the lack of a compressive force (P) (See Apps. 8-8,9,10).

Results show a maximum bending stress of 37.4 MPA at the base of the foot. Comparison to titanium's yield strength (Sy) of 661 MPa (@ 149 C) provides a safety factor of 17.7. With the maximum shear stress of 20.0 MPa at the tip of the foot, the factor of safety computed from the Maximum Shear Stress Theory is 16.5 (10). Similarly, deflection analysis

results in a deflection of -0.00001 m. Thus, the foot should be able to sustain any forces exerted from normal SKITTER operations and has a safety factor large enough to endure any unknown forces, including those resulting from maximum impact into the lunar soil.

CONCLUSION

The lunar utility vehicle SKITTER is in need of a foot apparatus to attach to the three femur-tibia design legs. The primary foot design is constrained to be of a ski-pole design that is compatible with the lunar environment and SKITTER functions.

The material chosen for the SKITTER foot is the titanium alloy Ti-6Al-4V. This alloy has an excellent strength to weight ratio and retains its strength at the extreme temperature ranges of the lunar environment. The alloy is also very corrosion and abrasion resistant.

The reduction of wear due to abrasion is necessary for a long service life of the foot. Thin, hard films are unacceptable in their present stage of development due to their inability to control abrasive wear. Hardfacing is an alternative that should work, but like the thin films, has not been tested at cryrogenic temperatures. Low stress loading will reduce abrasive wear; however, it does not meet the ski pole design constraint.

Research into thin films should lead to an increase in abrasive wear resistance in the future. Testing for delamination of the hard coating at high contact stresses, impact resistance, and effectiveness at cryrogenic temperatures also needs to be completed. Complex coatings should also offer properties superior to simple coatings in the near future.

The SKITTER foot must be able to perform for various angles of penetration and loads. The maximum load is considered to be the crane load, which occurs at an angle of 58 degrees to the horizontal. This load places a force of 27 kN in shear and 16.8 kN in compression on the foot. Impact forces were calculated for maximum free fall under maximum load. The results of the impact analysis were determined to be inconclusive due to unknown soil parameters.

An annulus attached to a pointed pole was the initial design for the SKITTER foot. Further design development resulted in a conical design with a disk at the top of the cone. Penetration would be resisted by the area of the cone, with the upper disk as a precaution for extreme sinkage. The cone (See Figure 11) is designed for 20 cm sinkage in average soil conditions, under maximum load. The weight of the three feet has been calculated to be 6.2% of the total weight.

The foot design was analyzed by two different methods; a deformable body analysis and a cantilever analysis. The deformable body analysis was used to determine the stresses and deflection of the foot in the crane position under crane loading. This analysis yielded stress levels far below the yield strength of the titanium, with insignificant deflection. The cantilever analysis used the actuator force applied to the foot in a vertical position for analysis. Once again, the analysis yielded stress levels well below the strength of the material, and the deflection was insignificant.

RECOMMENDATIONS

In designing and analyzing the SKITTER foot, several factors have arisen that will be important in future foot designs.

All fasets of our design led to the choice of titanium as the material from which to build the foot, due to its relatively light weight, high strength and toughness, and performance under extreme temperatures. The choice of Ti-10V-2Fe-3Al might prove to be of even more benefit because of its increased fatigue resistance. However, this type of titanium is relatively new, and cryogenic data is presently unavailable.

More knowledge of the various forces exerted on the foot is needed for accurate foot design. Specifically, more study is needed in the area of dynamic lunar soil penetration. Since no data was available for this analysis, numerous assumptions were made concerning the soil's damping characteristics. From calculations, this analysis might possibly yield some of the greatest forces on the SKITTER foot. With greater knowledge of forces and soil characteristics, the foot design might be possibly modified for weight savings.

Future research should involve further reduction of weight in the proposed foot design by additional hollowing of the center. A honeycomb core might also allow for a even lighter foot. A detailed internal stress evaluation should

then be completed for the foot.

For the present foot design, the tibia design could probably be modified to reduce stress at the point of connection to the foot. Such a change might involve joining two members at a point above the foot area and attaching the foot to a single member.

An alternative foot design was also conceived. The design uses a hemispherical bowl to spread out forces incident on the foot and increase the range from which forces could be applied on the foot. Traction for the foot could be provided by one or more spikes on the bottom of the bowl's convex surface. If supported correctly, the design might increase support with a minimum amount of frictional loss for the same weight as the present ski-pole design.

RECOMMENDATIONS FOR HARD COAT RESEARCH

At present, abrasion is the critical parameter which limits the use of thin films in a lunar application. Thus, it is recommended that research be conducted to increase the abrasion resistance of the hard coatings. Other mechanisms of wear such as adhesion and corrosion are not major factors in the foot design, so research can be focused solely on abrasive wear. When technology develops a hard coat which either reduces the hardness ratio to the .2 to .6 range or controls abrasion by other techniques, the thin films will be suitable for lunar use.

Other Hard Coat Research Recommendations

As of this date, there has been little research in the following areas: delamination of a hard coat due to high contact stresses, Impact resistance, and effectiveness at cryrogenic temperatures. The next step of hard coating evaluation for the SKITTER foot will be to conduct extensive research to satisfy these questions.

The possible delamination of a hard coat when high contact stresses are involved is a major concern. Since the SKITTER foot will be undergoing many different load configurations, numerous states of stress will occur. Unless research is conducted to ascertain that delamination will not result during high contact stress loading, then the hard coating techniques should not be used.

Impact resistance of a thin film needs to be researched in depth. When an object impacts another surface, the results could be elastic deformation, plastic deformation, or fracture. This is particularly important in regards to hard coatings. For the appropriate coating type and thickness to be selected, its resistance to film failure due to impact must be considered. In addition, research should be conducted to determine the possible detrimental effects of impact wear. Finally, these considerations must be correlated with the impact data of the substrate material.

The film integrity at various loadings in the cryrogenic

temperature range has not been observed. Since most of the common thin film applications have been for high temperature situations, the bulk of research has been confined to this area. In a lunar environment with temperatures as low as -200 degrees Celsius, possible delamination of the film could occur. Thus, extensive research must be conducted to scrutinize the effects of extremely low temperatures on the hard coatings.

BIBLIOGRAPHY

1. Sinton, W. M. "Temperatures of the Lunar surface." Physics and Astronomy of the Moon (S. Kopal, ed.), Academic Press, New York, ch. 11, 1972.

2. Schopf, J. W. "Micropaleontological studies of Lunar sample" California Univ. Jan. 1971. pp. 37.

3. Office of Technology Utilization National Aeronautics and Space Administration. "Surveyor Program Results." Washington D. C., 1969.

4. Mitchell, J. K. "Lunar Surface Engineering Properties Experiment Definition." et al. (California Univ.) Jan. 1971. pp. 38.

5. Peters, K. (Lamont-Doherty Geological Observatory) "Lunar Heat-Flow Experiment: Long term Temperature Observations on the Lunar surface at Apollo sites 15 and 17." Oct. 1975. pp. 35.

6. Surveyor I Mission Report. "Part II: Scientific Data and Results." (Jet Propulsion Lab., California Inst. of Tech.) Pasadena, Calif., Sep. 10, 1966.

7. Surveyor VII Mission Report. "Part II: Science Results." (Jet Propulsion Lab., California Inst. of Tech.) Pasadena, Calif., Mar. 15, 1968.

8. Chichka, Steven. et al., "Lunar Arthropod Leg Design," M. E. 4182, Spring Qtr., 1987.

9. Morris, James E. Lecture Notes from M. E. 3180 (Dr. W. M. Williams), 18 July, 1986. Referenced to Shigley and Mitchell, Chapter 2, pp.30-89.

10. Shigley, J. E. and L. D. Mitchell, Mechanical Engineering Design, Eqn. 3-3, p. 111.

11. Shigley, J. E. and L. D. Mitchell, Eqn. 6-1, p.226; Eqn 6-6,6-7, p. 232.

12. McMurray, G. V., and B. Mclaren. Personal interview. 28 July, 1987.

13. McMurray, G. V., and B. Mclaren. Personal interview. 6 August, 1987.

14. Wear Control Handbook. M. B. Peterson, W. O. Winer, 1980. A.S.M.E.

15. Frictional Behavior of Sputtered TIN. Yutaka Shimazaku, and W. O. Winer. Wear page 161 - 177. 1987.

16. Krushov, M. M. Principles of abrasive wear, page 28., 1987.

17. Tribological Properties of Marqnetron Sputtered Titanium Nitride. S. Camalignam, and W. O. Winer.

18. "On the Wear Behavior of PVD Ti, Al, Zr, V, N Coatings." Wear of Materials, 1987. Volume 2. A.S.M.E., pp. 551 - 556.

19. A.S.M. Handbook. A.S.M. 1987, pp. 12 -95.

20. Engel, Peter A. Impact Wear of Materials, Elserien Scientific Pub. Co., 1976.

21. Advanced Materials and Processes Guide to Selecting Engineering of Materials. June, 1987. A.S.M.

22. Askeland, Donald R. The Science and Engineering of Materials.

23. Eylon, Daniel, Titanium for Energy and Industrial Applications. Publication of the Metallurgical Society of A.I.M.E.

24. Heller, Martin E. Metal Selector Program.

Figure 1.

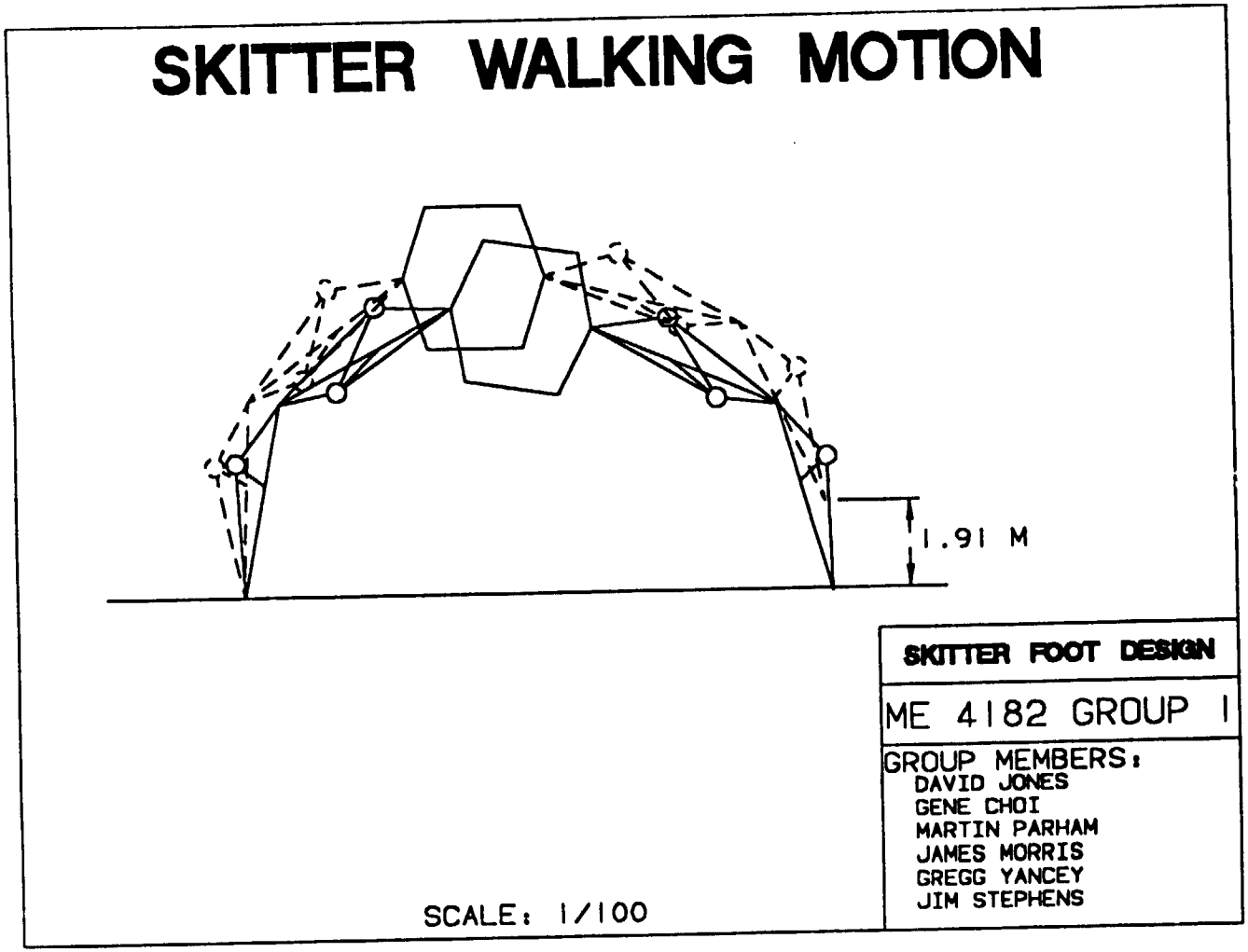
SKITTER WALKING MOTION
1.91 M
SKITTER FOOT DESIGN
ME 4182 GROUP 1
GROUP MEMBERS:
DAVID JONES
GENE CHOI
MARTIN PARHAM
JAMES MORRIS
GREGG YANCEY
JIM STEPHENS
SCALE: 1/100

Figure 2.

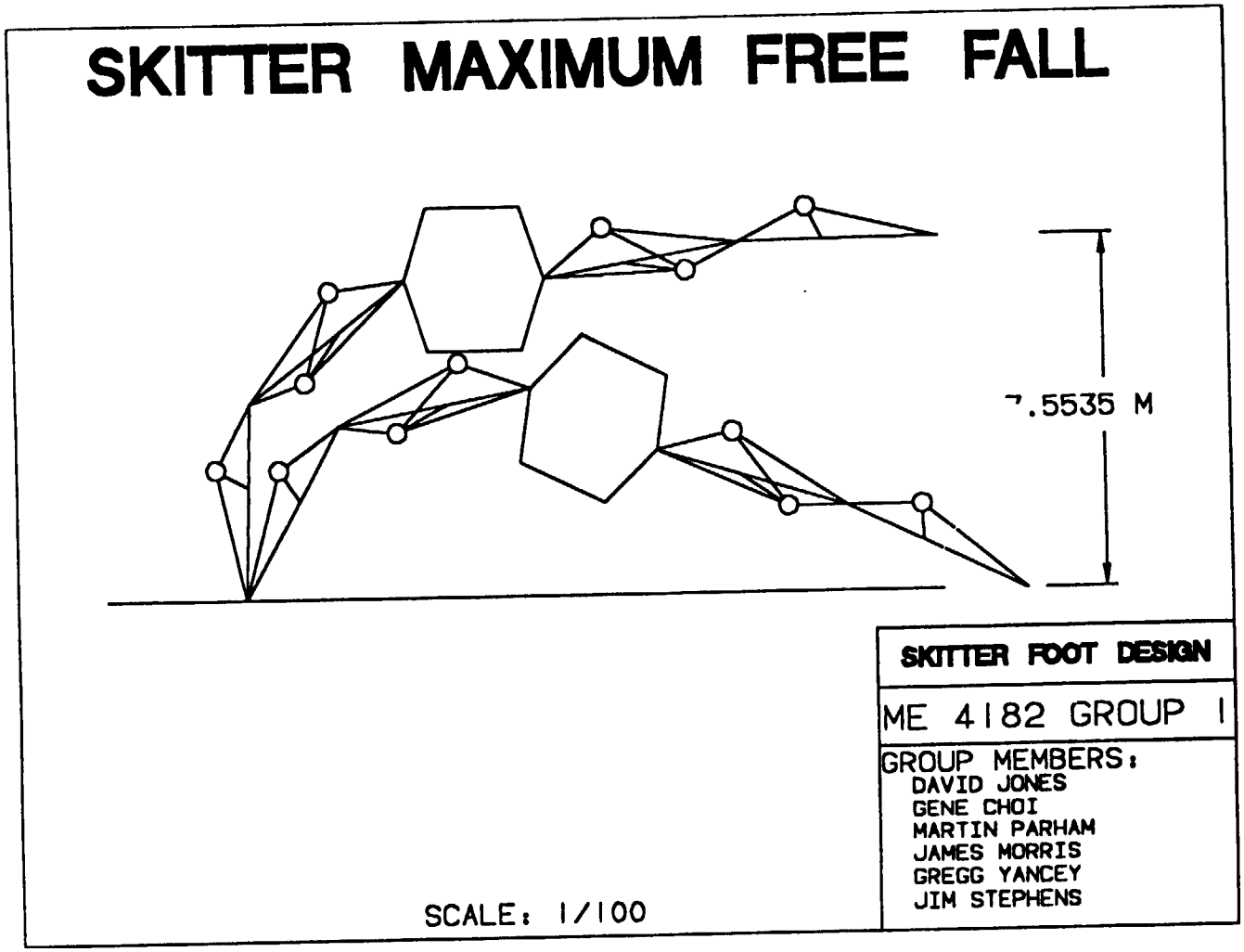
SKITTER MAXIMUM FREE FALL
7.5535 M
SKITTER FOOT DESIGN
ME 4182 GROUP 1
GROUP MEMBERS:
DAVID JONES
GENE CHOI
MARTIN PARHAM
JAMES MORRIS
GREGG YANCEY
JIM STEPHENS
SCALE: 1/100

Figure 3.

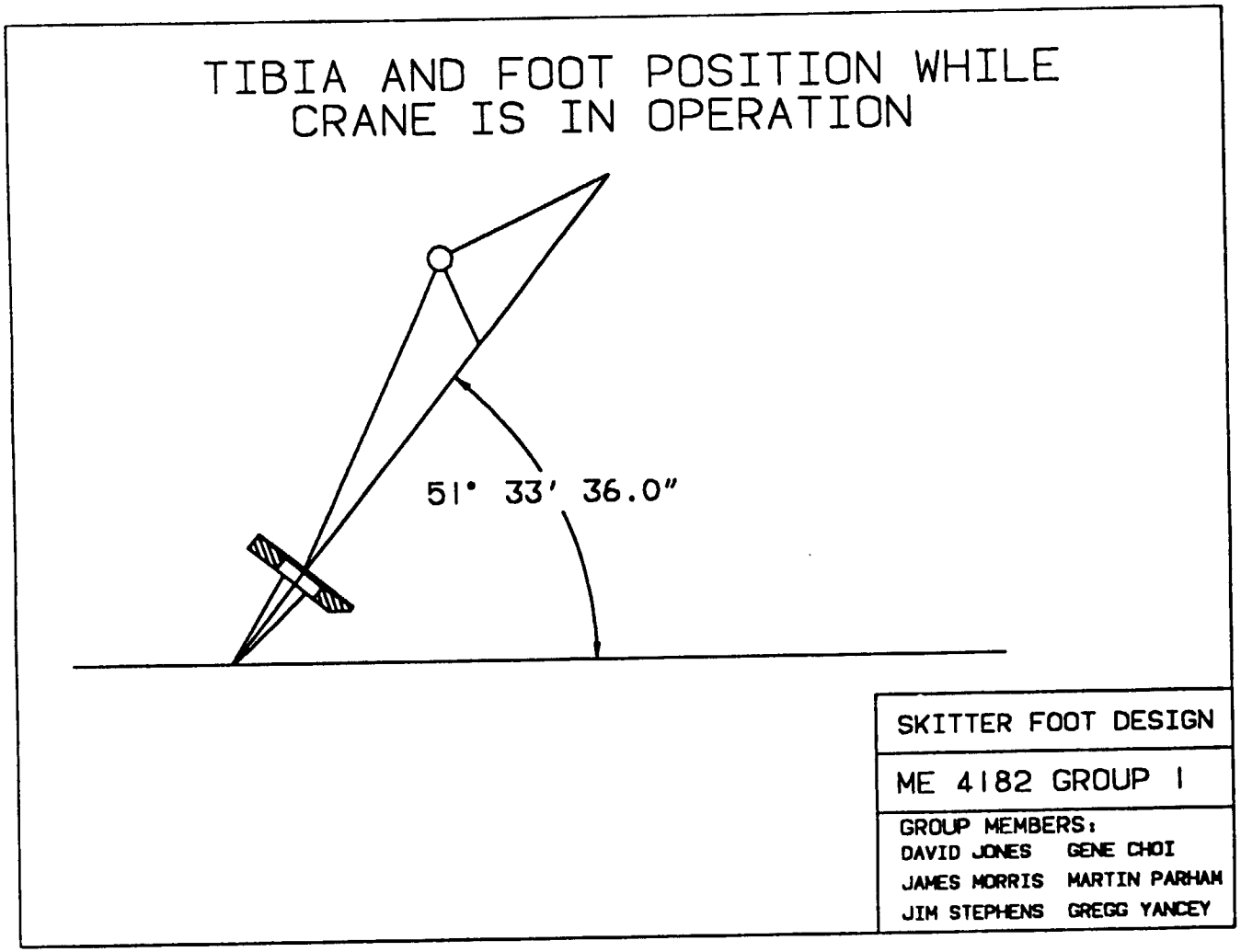
TIBIA AND FOOT POSITION WHILE CRANE IS IN OPERATION
51° 33' 36.0"
SKITTER FOOT DESIGN
ME 4182 GROUP 1
GROUP MEMBERS:
DAVID JONES GENE CHOI
JAMES MORRIS MARTIN PARHAM
JIM STEPHENS GREGG YANCEY

Figure 4.

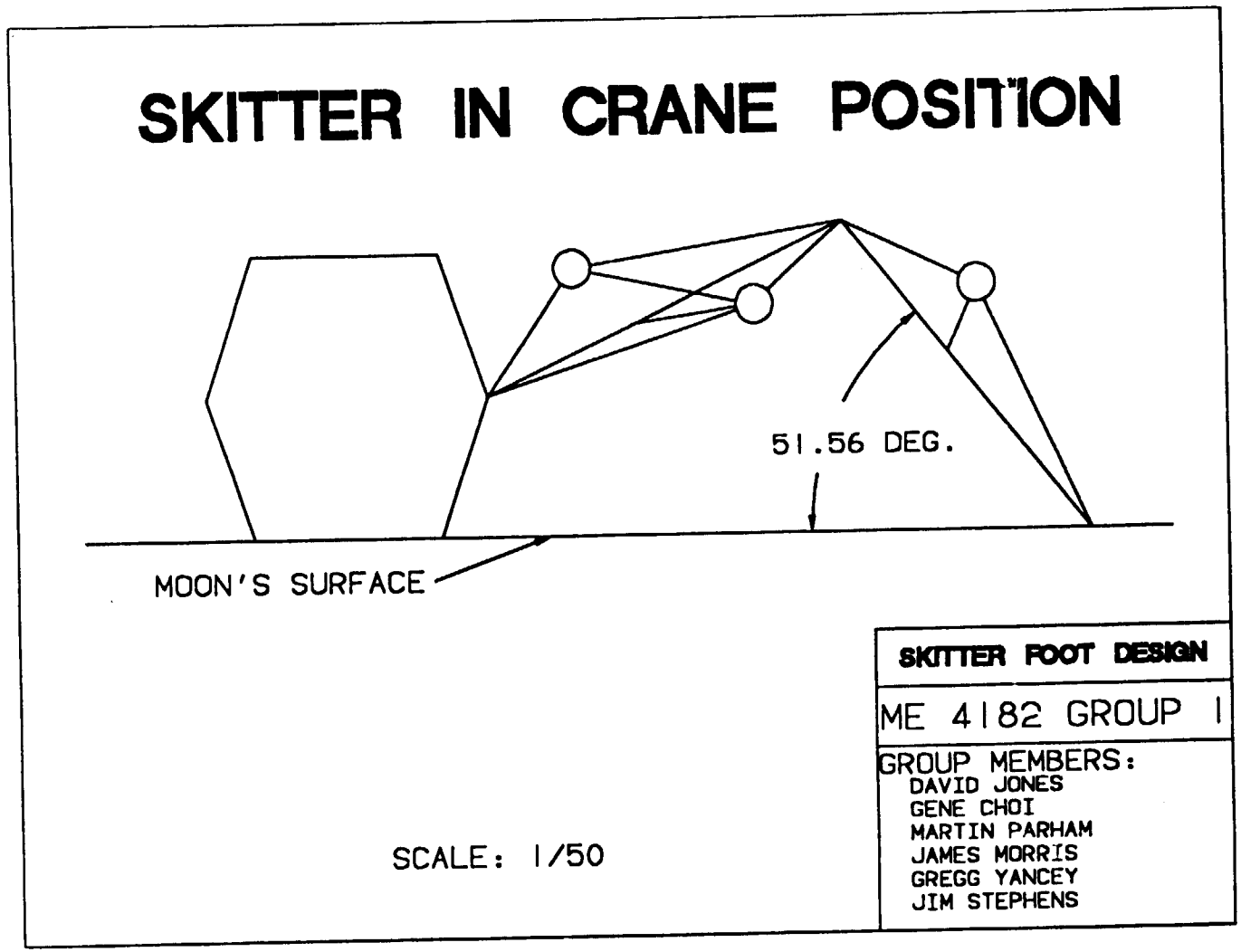
SKITTER IN CRANE POSITION
51.56 DEG.
MOON'S SURFACE
SKITTER FOOT DESIGN
ME 4182 GROUP 1
GROUP MEMBERS:
DAVID JONES
GENE CHOI
MARTIN PARHAM
JAMES MORRIS
GREGG YANCEY
JIM STEPHENS
SCALE: 1/50

Figure 5.

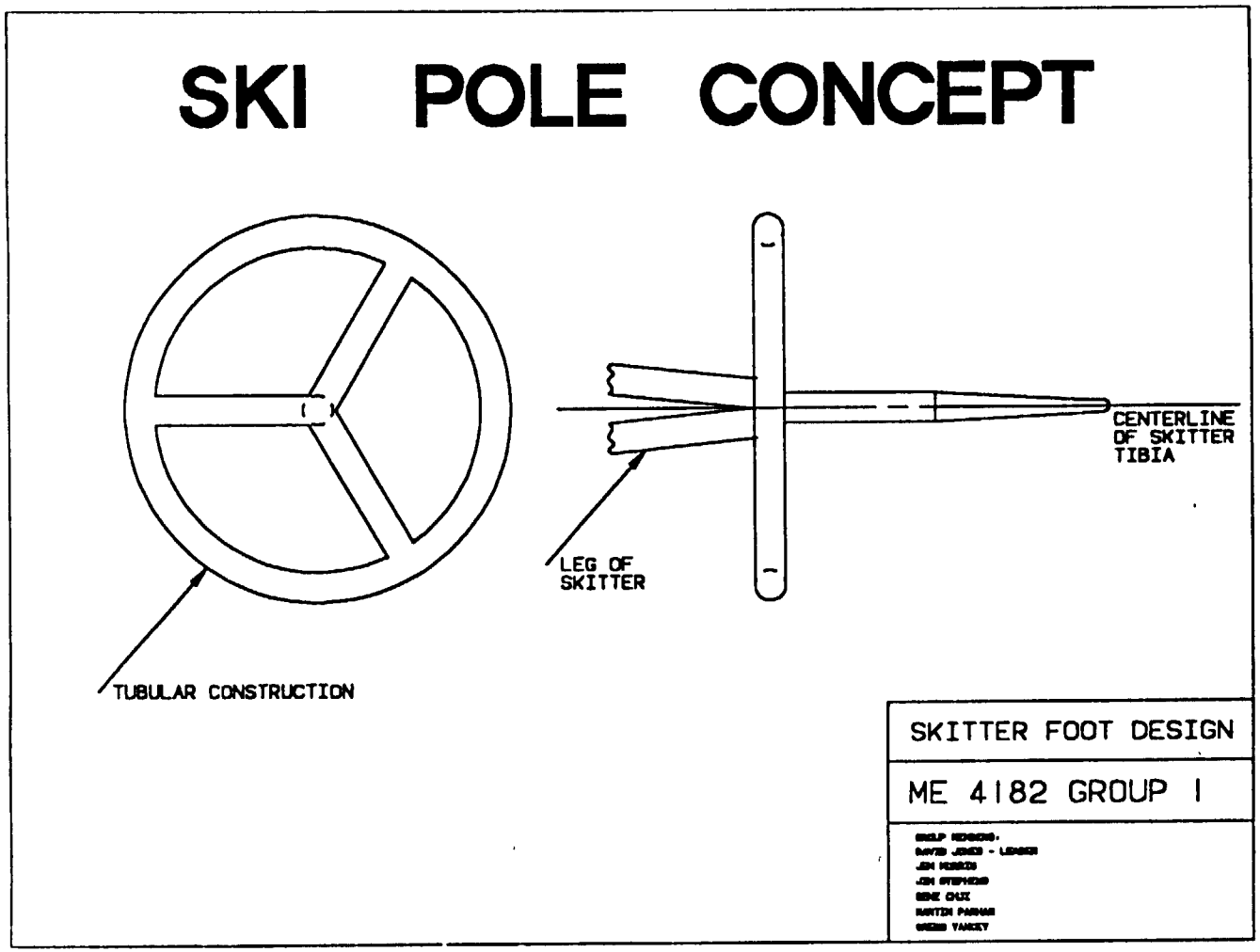
SKI POLE CONCEPT
CENTERLINE OF SKITTER TIBIA
LEG OF SKITTER
TUBULAR CONSTRUCTION
SKITTER FOOT DESIGN
ME 4182 GROUP 1

Figure 6.

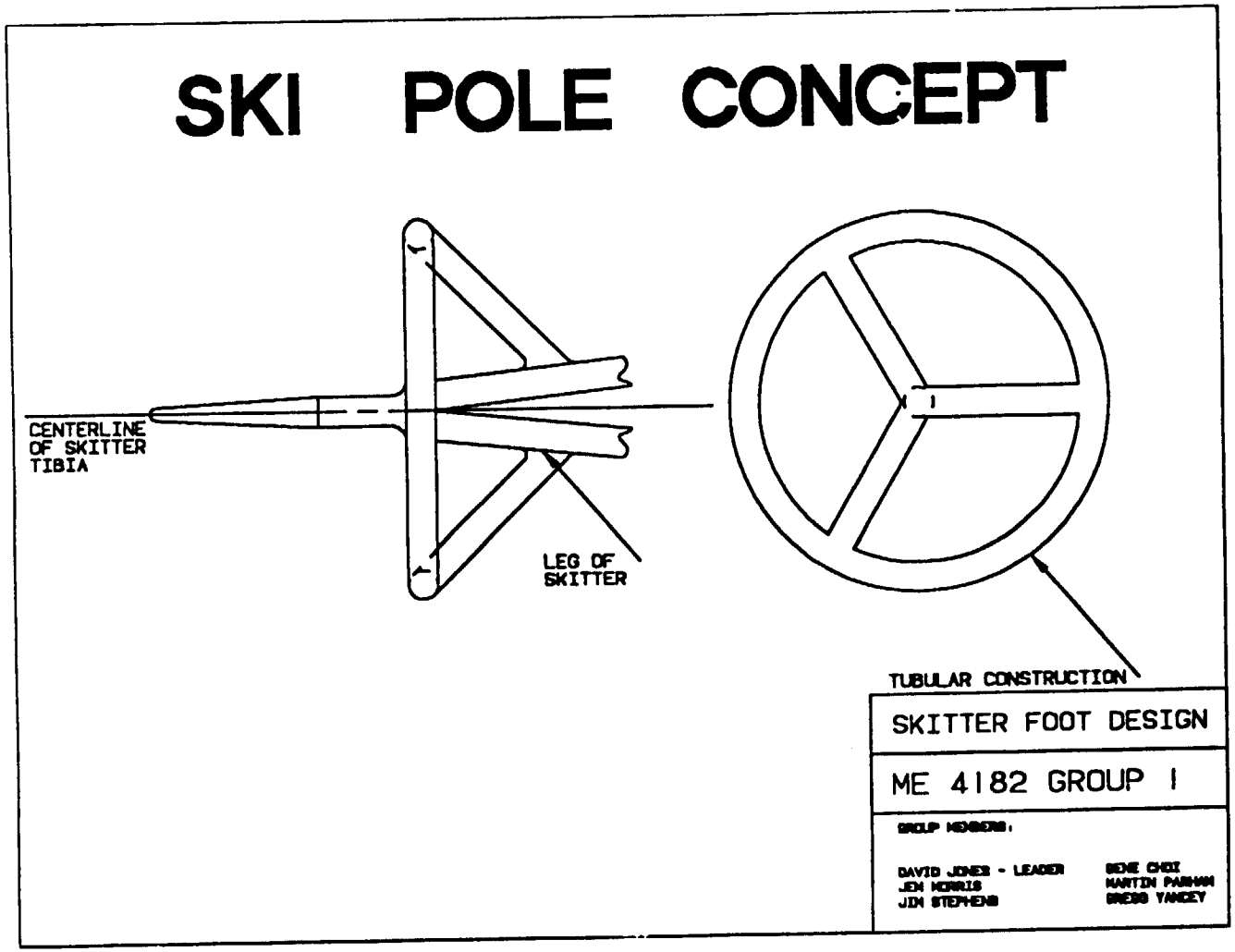
SKI POLE CONCEPT
CENTERLINE OF SKITTER TIBIA
LEG OF SKITTER
TUBULAR CONSTRUCTION
SKITTER FOOT DESIGN
ME 4182 GROUP 1
GROUP MEMBERS:
DAVID JONES - LEADER
JEN MORRIS
JIN STEPHENS
GENE CHOI
MARTIN PARHAM
GREGG YANCEY

Figure 7.

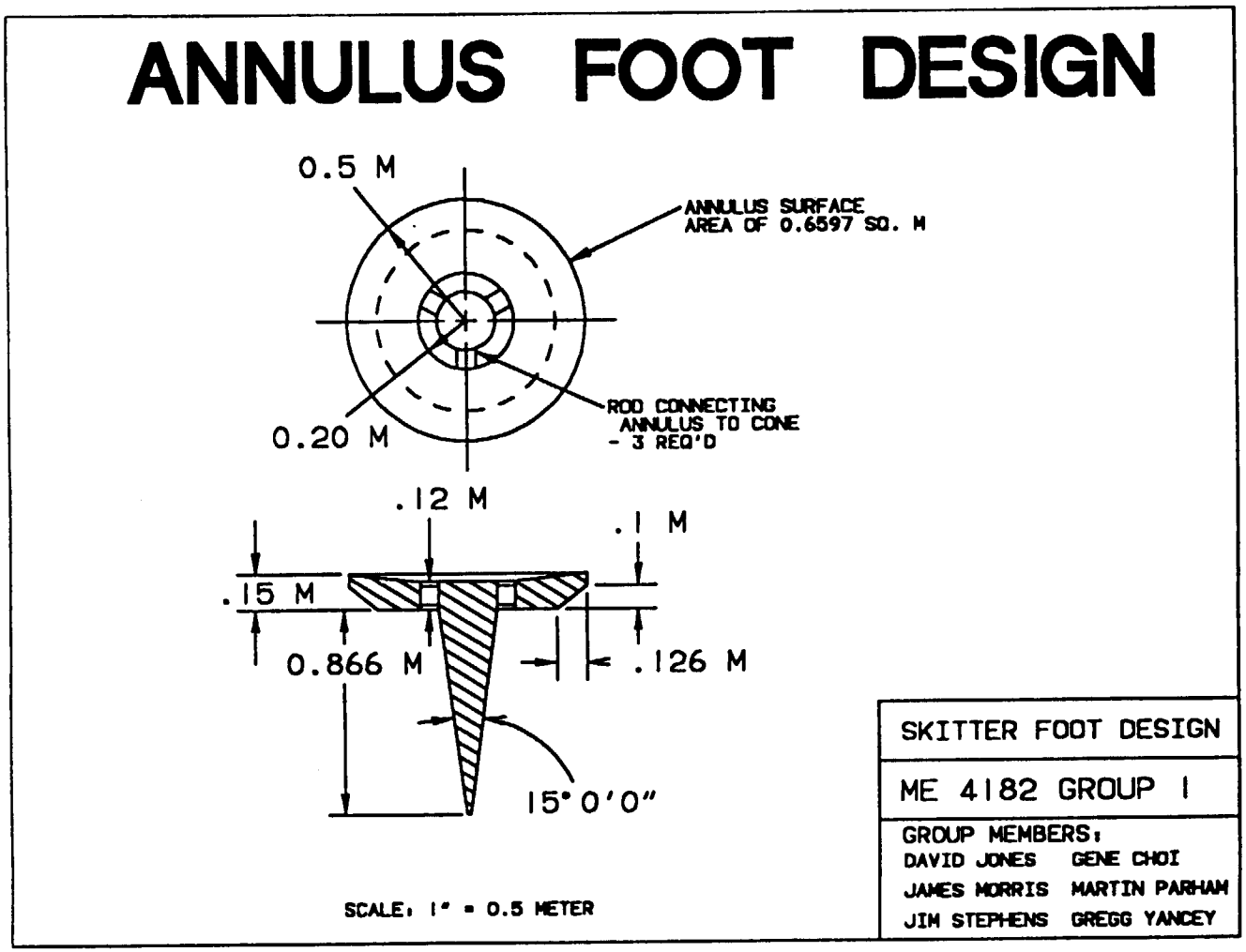
ANNULUS FOOT DESIGN
0.5 M
ANNULUS SURFACE
AREA OF 0.6597 SQ. M
ROD CONNECTING
ANNULUS TO CONE
- 3 REQ'D
0.20 M
.12 M
.1 M
.15 M
0.866 M
.126 M
15° 0' 0"
SCALE: 1" = 0.5 METER
SKITTER FOOT DESIGN
ME 4182 GROUP 1
GROUP MEMBERS:
DAVID JONES GENE CHOI
JAMES MORRIS MARTIN PARHAM
JIM STEPHENS GREGG YANCEY

Figure 8.

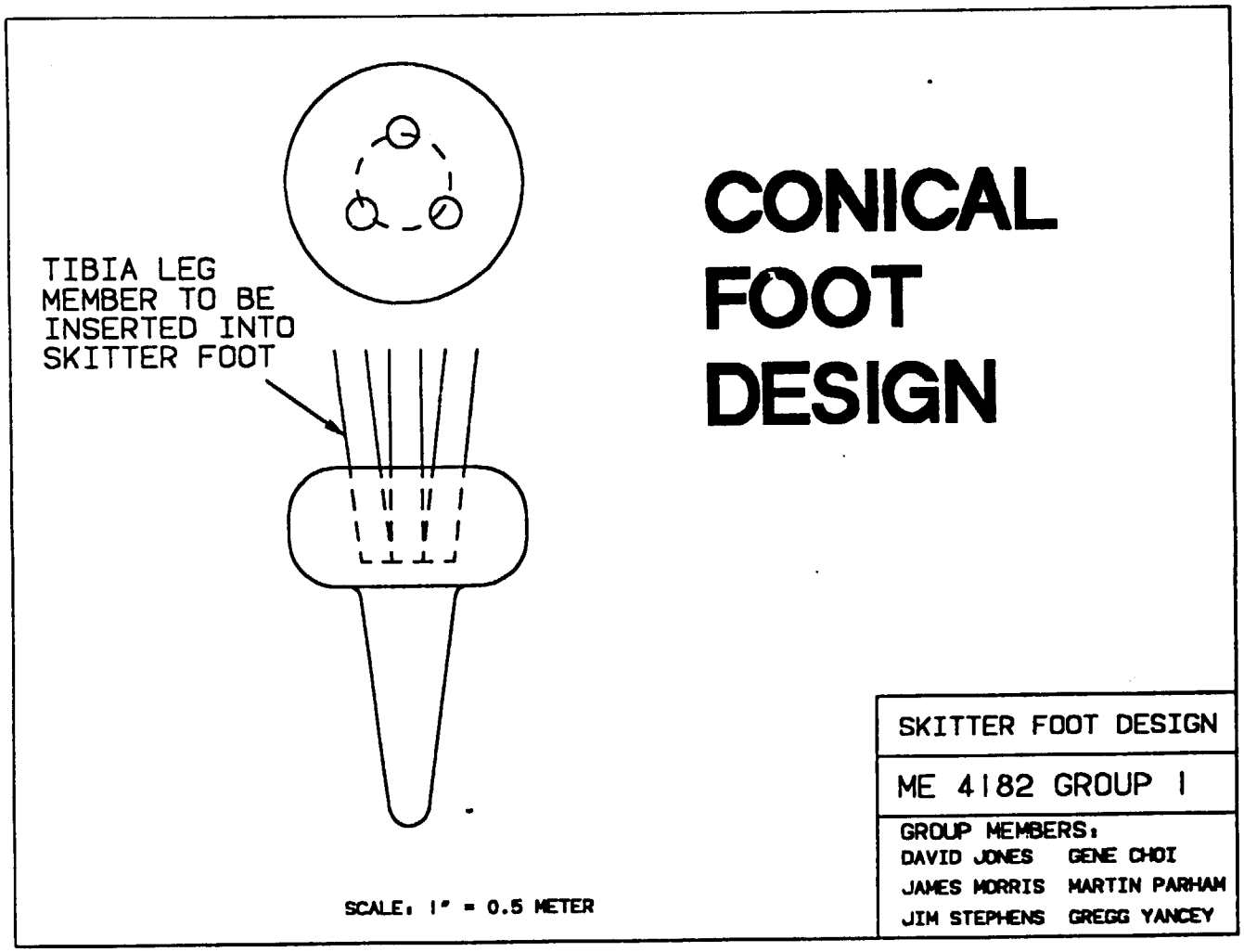
TIBIA LEG
MEMBER TO BE
INSERTED INTO
SKITTER FOOT
CONICAL
FOOT
DESIGN
SCALE: 1" = 0.5 METER
SKITTER FOOT DESIGN
ME 4182 GROUP 1
GROUP MEMBERS:
DAVID JONES GENE CHOI
JAMES MORRIS MARTIN PARHAM
JIM STEPHENS GREGG YANCEY

Figure 9.

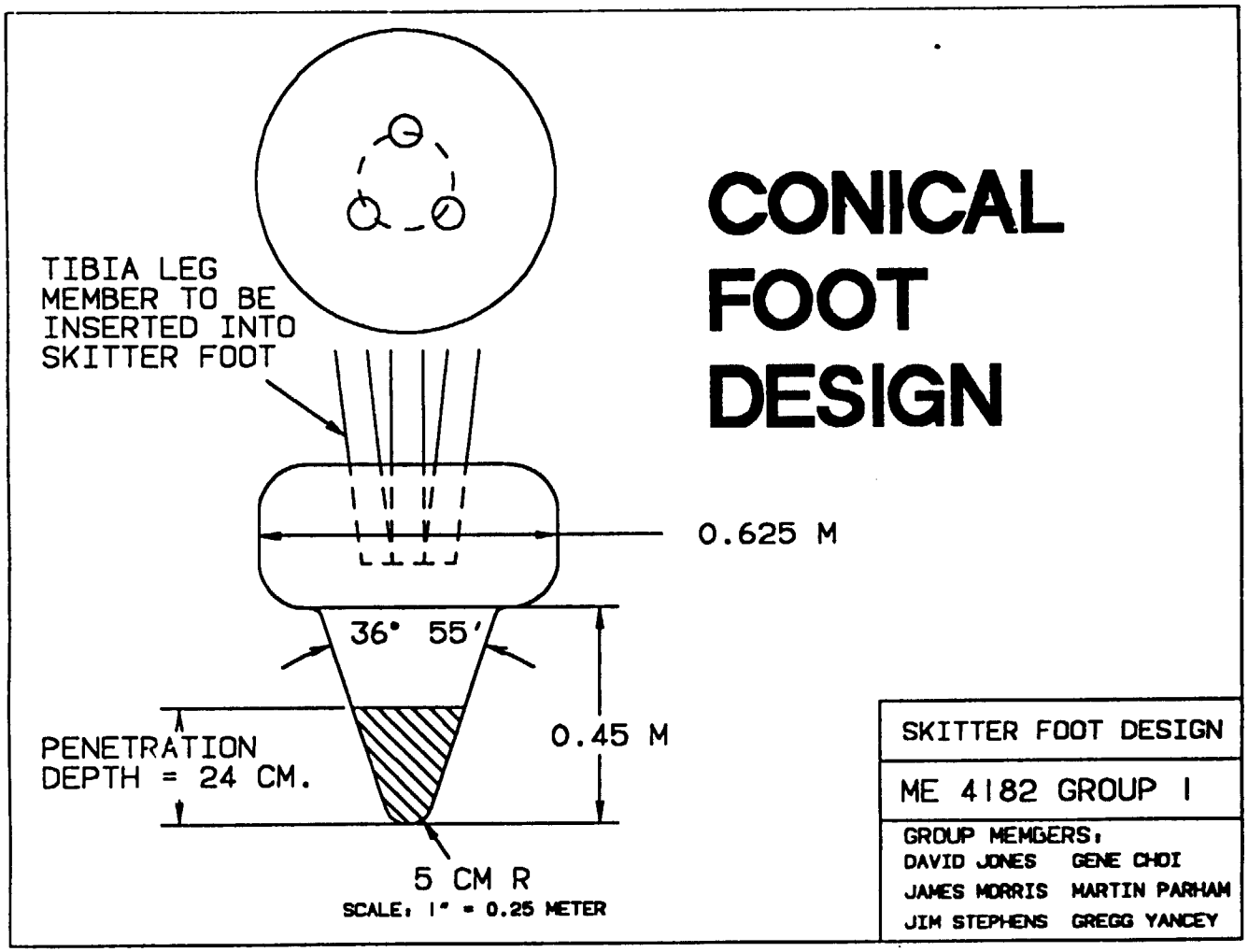
CONICAL FOOT DESIGN
TIBIA LEG MEMBER TO BE INSERTED INTO SKITTER FOOT
0.625 M
36° 55'
0.45 M
PENETRATION DEPTH = 24 CM.
5 CM R
SCALE: 1" = 0.25 METER
SKITTER FOOT DESIGN
ME 4182 GROUP 1
GROUP MEMBERS:
DAVID JONES GENE CHOI
JAMES MORRIS MARTIN PARHAM
JIM STEPHENS GREGG YANCEY

Figure 10.

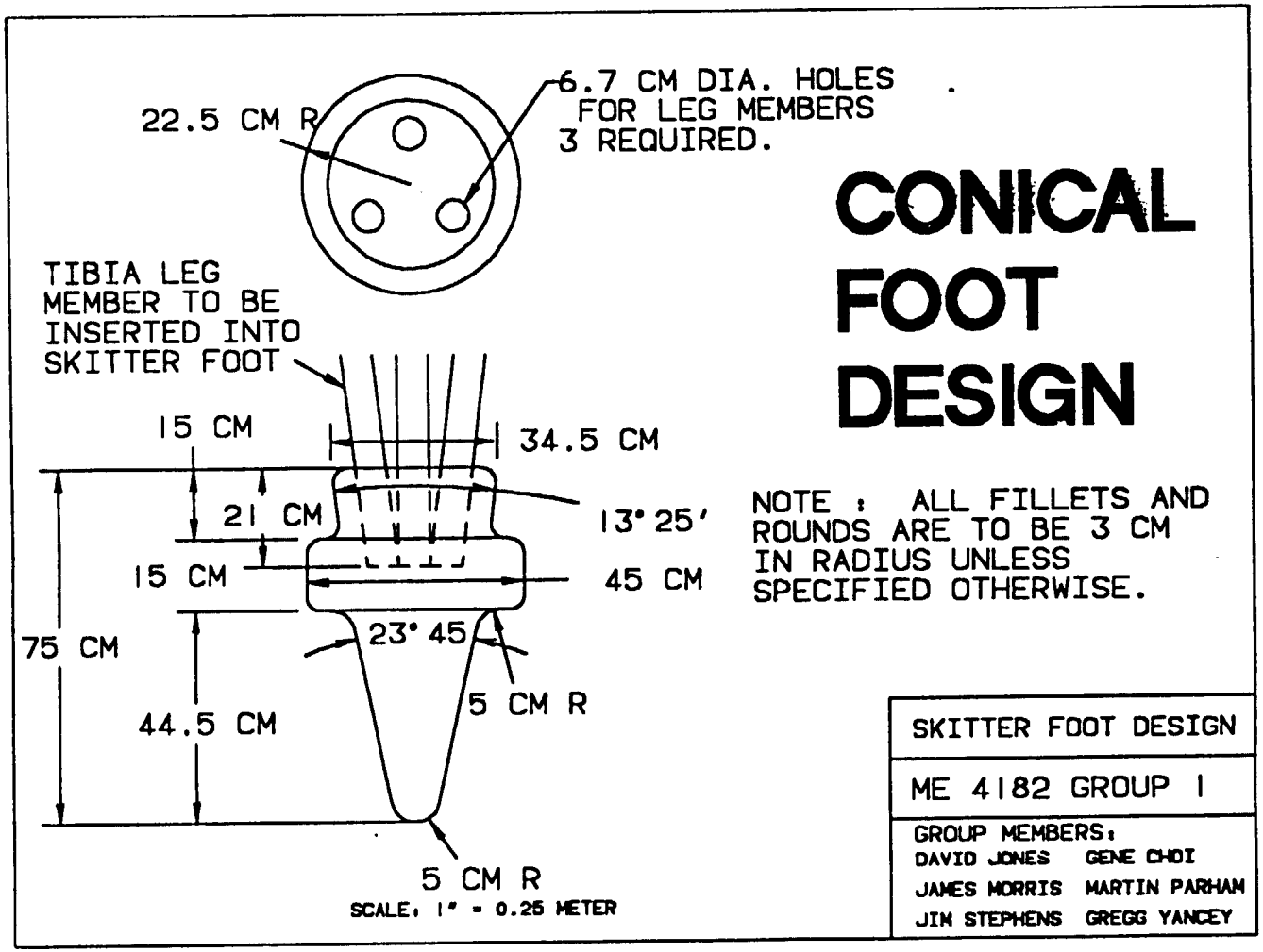
22.5 CM R
6.7 CM DIA. HOLES FOR LEG MEMBERS 3 REQUIRED.
CONICAL FOOT DESIGN
TIBIA LEG MEMBER TO BE INSERTED INTO SKITTER FOOT
15 CM
34.5 CM
21 CM
13° 25'
15 CM
45 CM
75 CM
23° 45
44.5 CM
5 CM R
5 CM R
SCALE: 1" = 0.25 METER
NOTE : ALL FILLETS AND ROUNDS ARE TO BE 3 CM IN RADIUS UNLESS SPECIFIED OTHERWISE.
SKITTER FOOT DESIGN
ME 4182 GROUP 1
GROUP MEMBERS:
DAVID JONES GENE CHOI
JAMES MORRIS MARTIN PARHAM
JIM STEPHENS GREGG YANCEY

Figure 11.

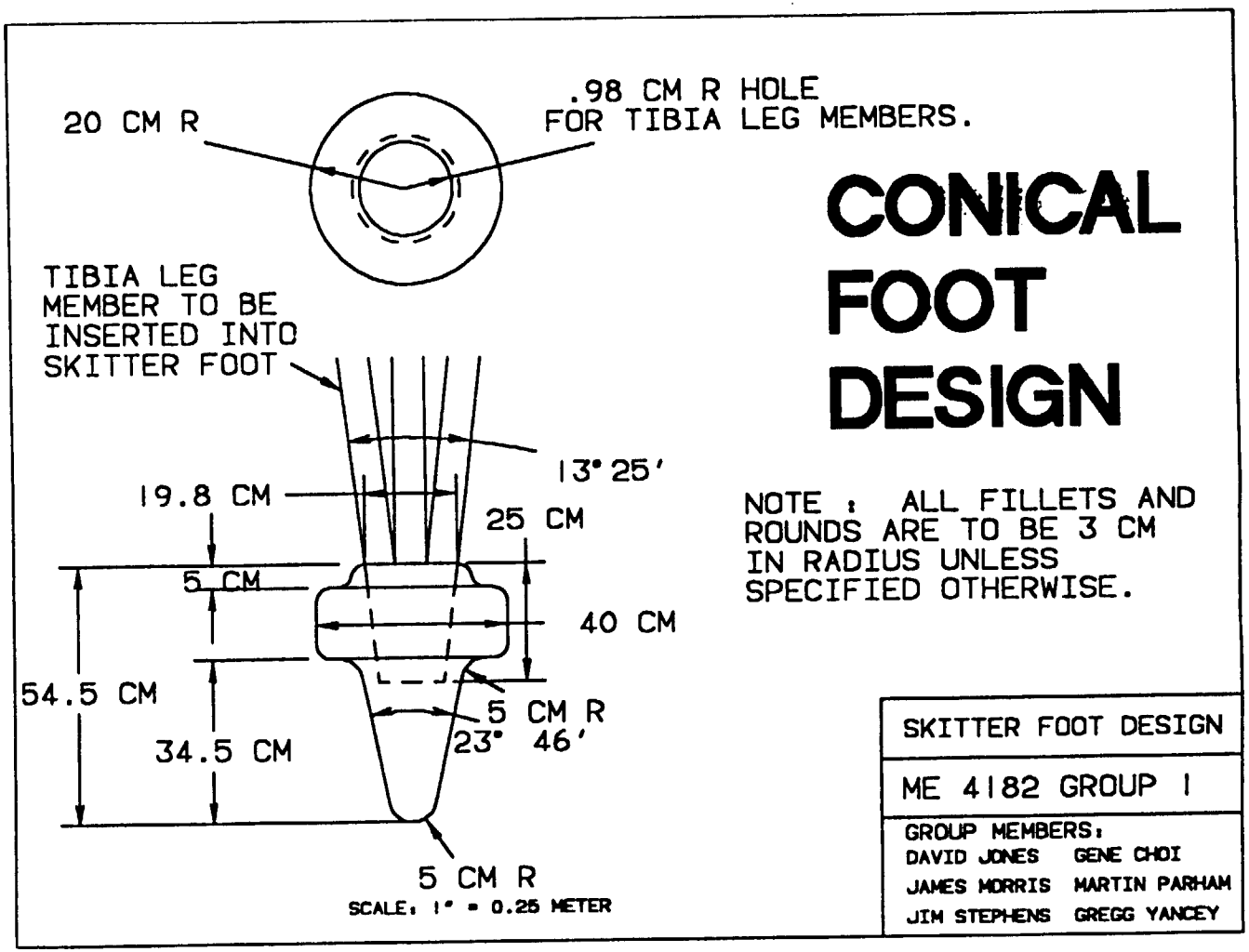
20 CM R
.98 CM R HOLE
FOR TIBIA LEG MEMBERS.
CONICAL
FOOT
DESIGN
TIBIA LEG
MEMBER TO BE
INSERTED INTO
SKITTER FOOT
13° 25'
19.8 CM
25 CM
5 CM
40 CM
54.5 CM
5 CM R
23° 46'
34.5 CM
5 CM R
SCALE: 1" = 0.25 METER
NOTE : ALL FILLETS AND
ROUNDS ARE TO BE 3 CM
IN RADIUS UNLESS
SPECIFIED OTHERWISE.
SKITTER FOOT DESIGN
ME 4182 GROUP 1
GROUP MEMBERS:
DAVID JONES GENE CHOI
JAMES MORRIS MARTIN PARHAM
JIM STEPHENS GREGG YANCEY

APPENDIX 4-1

FIG. 4.1

Typical tensile properties of Ti-6Al-4V

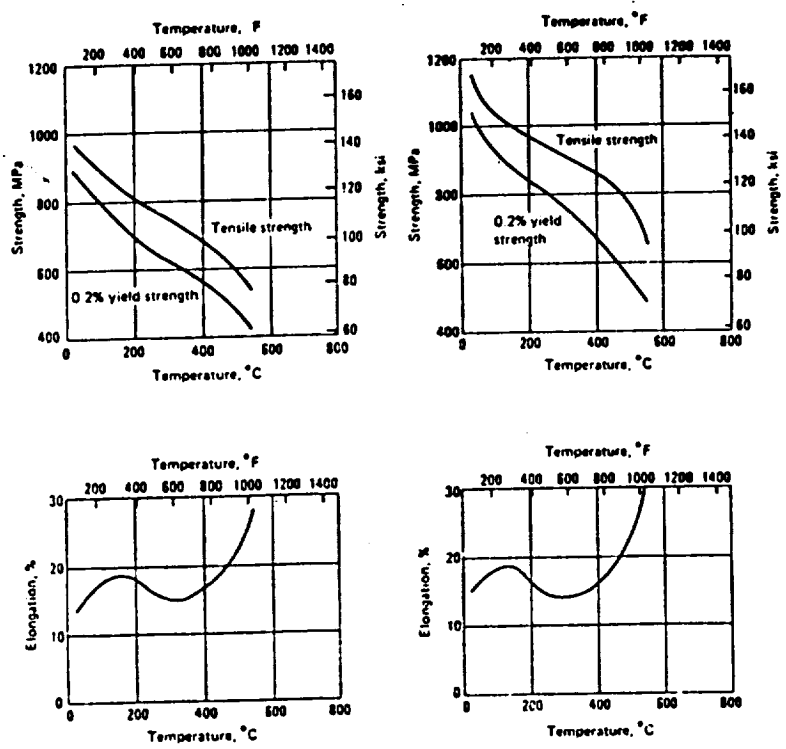

Left: Mill annealed condition. Right: STA condition—1 h at 955 °C (1750 °F), water quench, age 4 h at 525 °C (975 °F) and air cool.

Tensile properties vs temperature for round bars of Ti-10V-2Fe-3Al, STOA condition

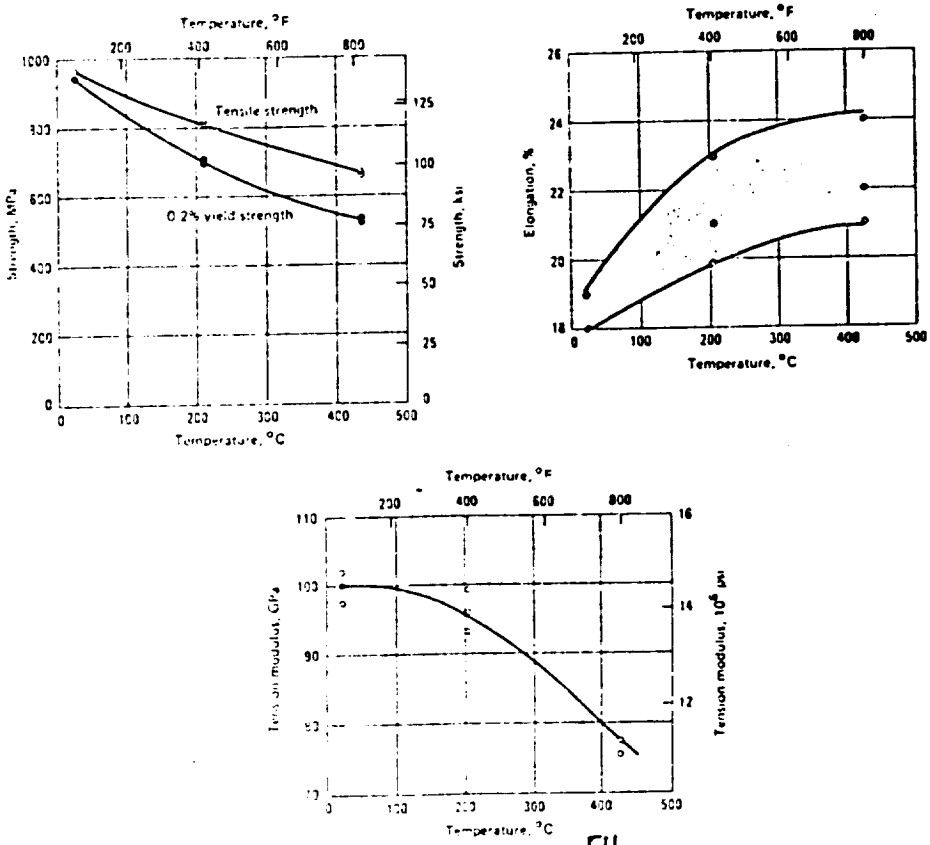

FIG. 4.2 **Creep-rupture data for Ti-6Al-4V bar**

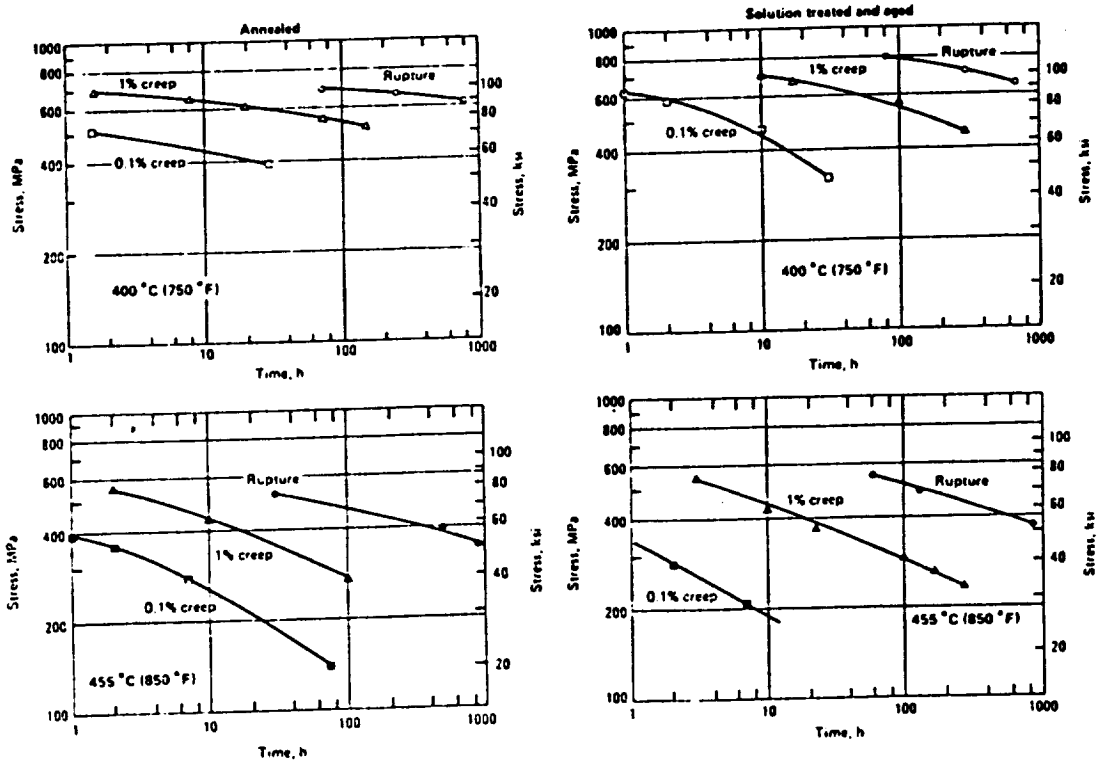

Creep and stress rupture curves for Ti-10V-2Fe-3Al, STA condition

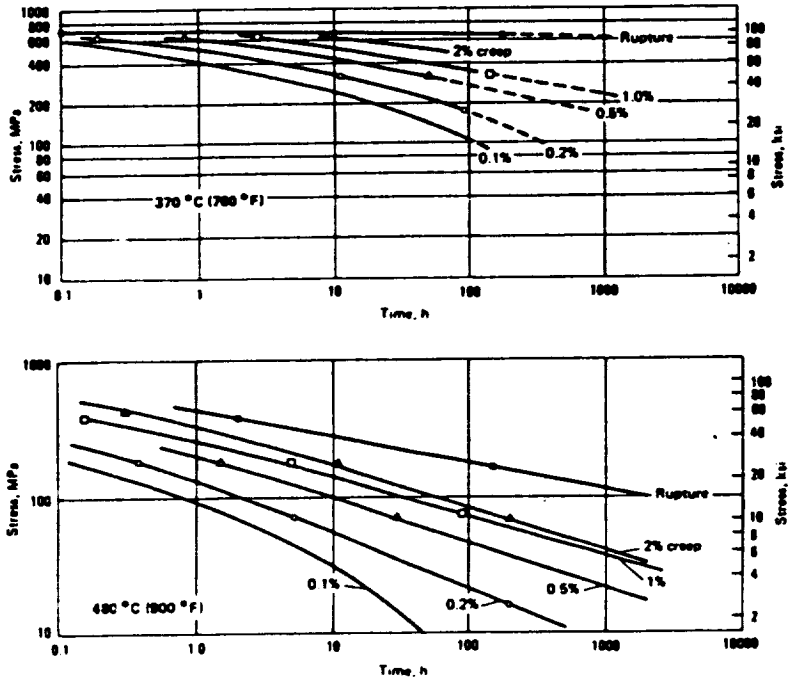

Data were determined from elevated temperature creep tests on round bars.

FIG. 4.3 **Typical rotating-beam fatigue curves for Ti-6Al-4V bar stock**

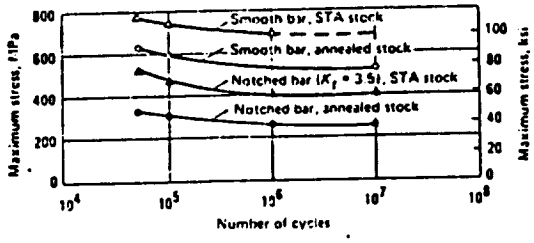

Axial fatigue of Ti-10V-2Fe-3Al bar stock in the STOA condition

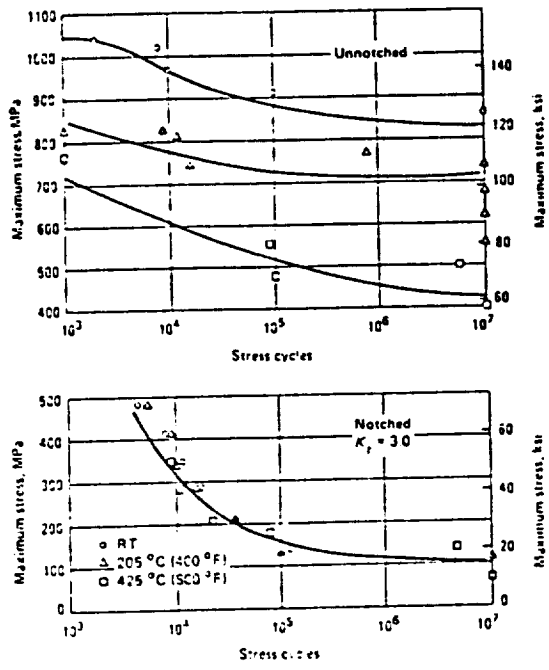

Specimens were taken from round bars 75 mm (3 in.) in diameter that had been solution treated 1 h at 760 °C (1400 °F), furnace cooled, overaged 8 h at 565 °C (1050 °F) and air cooled. Tests were conducted at a stress ratio of $R = 0.1$ and a frequency of 20 Hz.

FIG. 4.4

Plane-strain fracture toughness vs tensile strength for Ti-10V-2Fe-3Al forgings

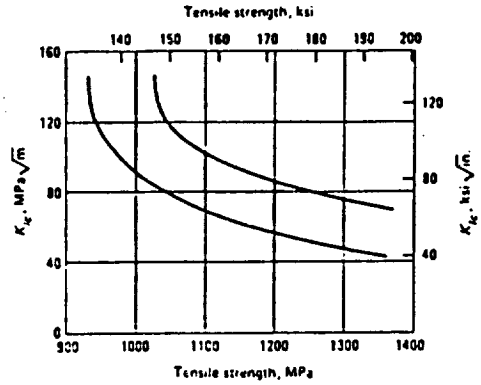

Data represent a composite of fracture toughness values for beta-forged die forgings, beta-forged block forgings, and beta forged plus alpha-beta-forged die forgings.

Mean coefficient of thermal expansion for Ti-6Al-4V

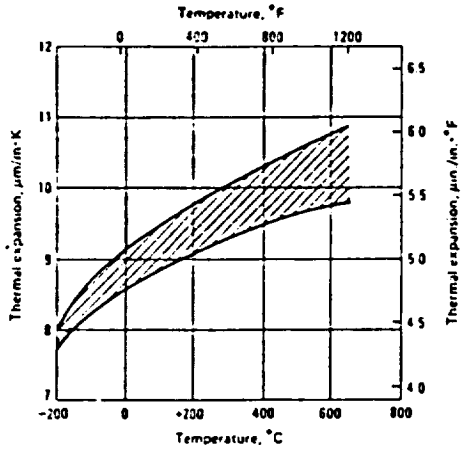

Expansion data are for room temperature to indicated temperature for both mill annealed and solution treated and aged stock.

FIG. 4.5

Young's modulus for Ti-5Al-2.5Sn and Ti-6Al-4V alloys as determined ultrasonically (Ref 95)

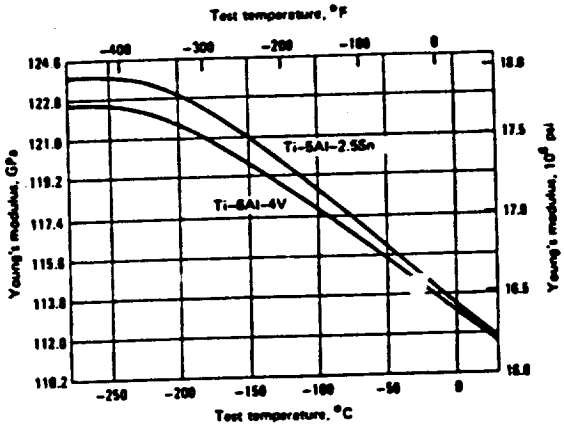

Poisson's ratios for Ti-5Al-2.5Sn and Ti-6Al-4V alloys as determined ultrasonically (Ref 95)

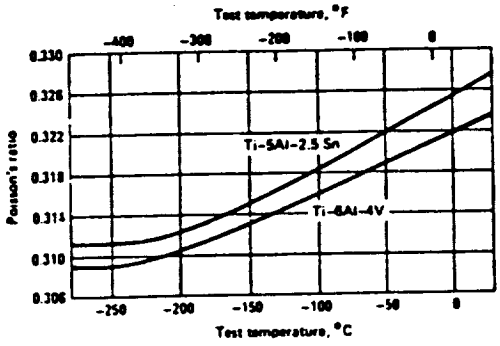

Data from Ref 2, 7, 14, 44, 60, 89-93

TABLE 4.3

App. 4-6

Temperature °C	Temperature °F	Tensile strength MPa	Tensile strength ksi	Yield strength MPa	Yield strength ksi	Elongation, %	Reduction in area, %	Notch tensile strength(a) MPa	Notch tensile strength(a) ksi	Young's modulus GPa	Young's modulus 10^6 psi
Ti-75A sheet, annealed, longitudinal orientation											
24	75	580	84.3	465	67.6	25	...	785	114	...	...
-78	-108	750	109	615	89.2	25	...	...	...	...	...
-196	-320	1050	152	940	136	18	...	1100	159	...	...
-253	-423	1280	186	1190	173	8	...	875	127	...	...
Ti-75A sheet, annealed, transverse orientation											
24	75	585	85.1	475	69.0	25	...	800	116	...	...
-78	-108	760	110	645	93.4	20	...	905	131	...	...
-196	-320	1060	153	965	140	14	...	1120	163	...	...
-253	-423	1340	194	1260	182	7	...	880	128	...	...
Ti-5Al-2.5Sn sheet, nominal interstitial annealed, longitudinal orientation											
24	75	850	123	795	115	16	...	1130	164	105	15.4
-78	-108	1080	156	1020	148	13	...	1310	190	115	16.6
-196	-320	1370	199	1300	188	14	...	1630	236	120	17.7
-253	-423	1700	246	1590	231	7	...	1430	208	130	18.5
Ti-5Al-2.5Sn sheet, nominal interstitial annealed, transverse orientation											
24	75	895	130	860	125	14	...	1170	170	...	...
-78	-108	1050	152	1020	148	12	...	1250	181	...	...
-196	-320	1430	208	1370	198	12	...	1630	236	...	...
-253	-423	1670	242	1610	234	6	...	1290	187	...	...
-268	-450	1590	231	...	...	1.5	...				
Ti-5Al-2.5Sn (ELI) sheet, annealed, longitudinal orientation											
24	75	800	116	740	107	16	...	1060	154	115	16.4
-78	-108	960	139	860	125	14	...	1190	173	125	18.0
-196	-320	1300	188	1210	175	16	...	1560	226	130	18.6
-253	-423	1570	228	1450	210	10	...	1670	242	130	19.2
Ti-5Al-2.5Sn (ELI) sheet, annealed, transverse orientation											
24	75	805	117	760	110	14	...	1100	159	110	16.0
-78	-108	950	138	895	130	12	...	1260	182	125	18.1
-196	-320	1300	188	1230	179	14	...	1570	228	130	18.9
-253	-423	1570	228	1480	214	8	...	1530	222	140	20.1
Ti-5Al-2.5Sn (ELI) sheet/weldment, annealed, EB weld											
24	75	815	118	785	114	...	...	...	...	...	...
-196	-320	1300	189	1210	176	...	...	...	...	...	...
-253	-423	1510	219	1380	200	...	...	...	...	...	...
Ti-5Al-2.5Sn (ELI) plate, annealed, longitudinal orientation											
24	75	765	111	705	102	33	43	...	...	...	...
-253	-423	1430	208	1390	202	17	32	...	...	...	...
Ti-5Al-2.5Sn (ELI) forgings, as forged, tangential orientation											
24	75	835	121	760	110	15	36	...	...	...	...
-78	-108	980	142	905	131	12	31	...	...	...	...
-196	-320	1260	182	1100	159	15	30	...	...	...	...
-253	-423	1420	206	1260	182	13	22	...	...	...	...
Ti-6Al-4V (ELI) sheet, annealed, longitudinal orientation											
24	75	960	139	890	129	12	...	1120	162	110	16.2
-78	-108	1160	168	1100	160	9	...	1220	177	115	16.6
-196	-320	1500	217	1420	206	10	...	1460	211	120	17.5
-253	-423	1770	256	1700	246	4	...	1500	217	130	18.6
Ti-6Al-4V (ELI) sheet, annealed, transverse orientation											
24	75	960	139	895	130	12	...	1130	164	110	16.0
-78	-108	1170	169	1100	160	12	...	1260	183	115	16.5
-196	-320	1500	218	1460	212	11	...	1440	209	125	18.2
-253	-423	1750	254	1700	246	4	...	1550	225	130	19.2
Ti-6Al-4V (ELI) plate, annealed, longitudinal orientation											
24	75	890	129	840	122	15	37	...	...	...	...
-253	-423	1640	238	1600	232	...	8	...	...	...	...
Ti-6Al-4V (ELI) forgings, as forged, longitudinal orientation											
24	75	970	141	915	133	14	40	1330	193	...	...
-78	-108	1160	168	1120	163	13	31	1560	226	...	...
-196	-320	1570	227	1480	214	11	31	1900	276	...	...
-253	-423	1650	239	1570	227	11	24	1820	264	...	...
Ti-6Al-4V (ELI) forging, recrystallization annealed(b)											
24	75	890	129	825	120	14	41	...	...	110	16.1
-196	-320	1430	207	1370	198	10	16			120	17.5

(59)

APPEND. 4-7

LE. 4.4 **Results of fatigue-life tests on two titanium alloys**

Data from Ref 41, 42, 49, 50

Alloy and condition	Stressing mode	Stress ratio, R	K_t	Fatigue strengths at 10^5 cycles 24 °C (75 °F) MPa	ksi	−196 °C (−320 °F) MPa	ksi	−253 °C (−423 °F) MPa	ksi
Ti-5Al-2.5Sn (ELI) sheet, annealed	Axial	0.01	1	495	72	815	118	760	110
			3.5	220	32	205	30	160	23
Ti-5Al-2.5Sn (ELI) sheet(a)	Axial	0.01	1	485	70	565	82	425	62
Ti-5Al-2.5Sn (ELI) bar, annealed(b)	Axial	0	1	760	110	985	143	925	134
Ti-6Al-4V (ELI) sheet(c)	Axial	0.01	1	505	73	675	98	895	130
			3.5	285	41	295	43	275	40
Ti-6Al-4V (ELI) sheet(a)	Axial	0.01	1	600	87	595	86	560	81
Ti-6Al-4V sheet, annealed	Flex	−1.0	1	345	50	550	80	530	77
			3.1	170	25	185	27	255	37

(a) Gas tungsten arc welded, base metal filler. (b) Cyclic frequency, 28 Hz. (c) STA: 900 °C (1650 °F) 5 min, WQ; 540 °C (1000 °F) 4 h, AC.

Fatigue-crack-growth rates for Ti-5Al-2.5Sn and Ti-6Al-4V (Ref 61)

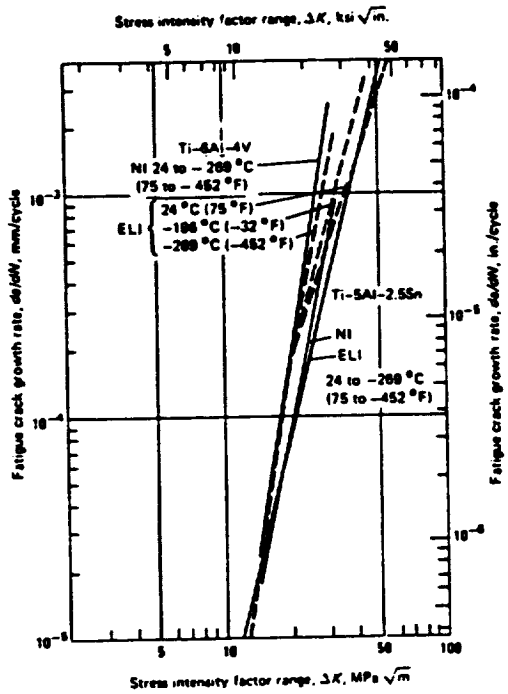

NI = normal interstitial content; ELI = extra-low interstitial content. See Table 50 for C and n values for fatigue-crack-growth rate equations.

LE. 4.5

cture toughness of two titanium alloys and weldments

oy and dition(s)	Form	Room temperature yield strength MPa	ksi	Specimen design	Orientation	Fracture toughness, K_Q 24 °C(75 °F) MPa$\sqrt{m}$	ksi$\sqrt{in.}$	−196 °C(−320 °F) MPa$\sqrt{m}$	ksi$\sqrt{in.}$	−253 °C(−423 °F) MPa$\sqrt{m}$	ksi$\sqrt{in.}$	−269 °C(−452 °F) MPa$\sqrt{m}$	ksi$\sqrt{in.}$
5Al-5Sn(NI), nealed	Plate	876	127	CT	L-T	71.8	65.4	53.4	48.6	...	...	...	...
		876	127	Bend	L-T	...	...	...	...	51.4	46.8	...	...
		876	127	Bend	L-S	...	...	...	...	50.2	45.7	...	...
	Bar	871	126	CT	T-S	77.2	70.3	42.1	38.3	...	...	42.0	38.2
5Al-5Sn(ELI), nealed	Plate	703	102	CT	L-T	...	...	111	101	...	...	...	...
		703	102	Bend	L-T	...	...	...	...	69.6	81.5	...	...
5Al-5Sn(ELI), forged	Forging	760	110	CT	R-L	...	...	...	...	79.4	72.3	...	...
					R-C	...	...	...	...	58.5	53.2	...	...
5Al-5Sn(ELI)	Forging(b)	779	113	CT	...	...	...	...	...	54.4 to 75.3	49.5 to 68.5	...	...
6Al-4V D), an-aled	Bar	942	136	CT	T-L	47.4	43.2	38.8	35.3	...	...	38.5	35.1
6Al-4V LI), as ged	Forging	830	120	CT	T-L	...	...	61.0	55.5	...	...	54.1	49.2
6Al-4V D,	Forging	830	120	CT	M-L(c)	...	...	62.8	57.2	...	...	...	...
					M-R(c)	...	...	62.0	56.4	...	...	...	...
6Al-4V LI, , electron eam elded, SR	Forging	830	120	CT	M-R(c)	...	...	61.1(d)	55.6(d)	...	...	...	...
	Weldment	...	...	...	M-L(c)	...	...	56.9(d)	51.8(d)	...	...	...	...
					M-R(c)	...	...	57.1(e)	52.0(e)	...	...	...	...
					M-R(c)	...	...	51.0(f)	46.4(f)	...	...	...	...

R = stress relieved: 540 °C (1000 °F) 50 h, AC. FC = furnace cool. AC = air cool. NI = normal interstitial content. ELI = extra low interstitial content. RA crystallization annealed: 930 °C (1700 °F) 4 h, FC to 810 °C (1400 °F) in 3 h, cooled to 480 °C (900 °F) in 3/4 h, AC. (b) Range for 18 tests. (c) M-L and M-R are ific orientations in a spherical forging. (d) Fusion zone. (e) Heat affected zone. (f) Heat affected zone boundary.

APPENDIX 5-1

MICROHARDNESS OF TYPICAL HARD COAT MATERIALS (2)

VICKERS HARDNESS, kg/mm^2

ELEMENT	Carbide	Nitride	Boride
BORON	3700	--	--
CHROMIUM	1600-Cr7C3 1300-Cr3C2	2200 1083-CrN	1800
HAFNIUM	2270-2650	1640	2250-2900
MOLYBEDNUM	1800-MoC	--	2350
NIOBIUIM	2400-2850	1396-NbN 1720-Nb2N	2100-2400
SILICON	3500	--	--
TANTALUM	1800-2450	--	--
TITANIUM	2000-3000	1200-2000	2200-3500
TUNGSTEN	2100-2400 1450-W2C	--	2400-2660
VANADIUM	2460-3150	1520-1900	2070-2800
ZIRCONIUM	2360-2600	1150	2250-2600

NOTE: Literature microhardness values span a moderately wide range. A single specific value is usually not representative. Transition metal oxides, nitrides, and carbides can vary widely in stoichiometry and are mutually soluble. Variations in hardness reported are due to variations in stoichiometry and purity. Most borides, especially the hexogonal borides, are highly anisotropic.

FORCES INCIDENT ON FOOT

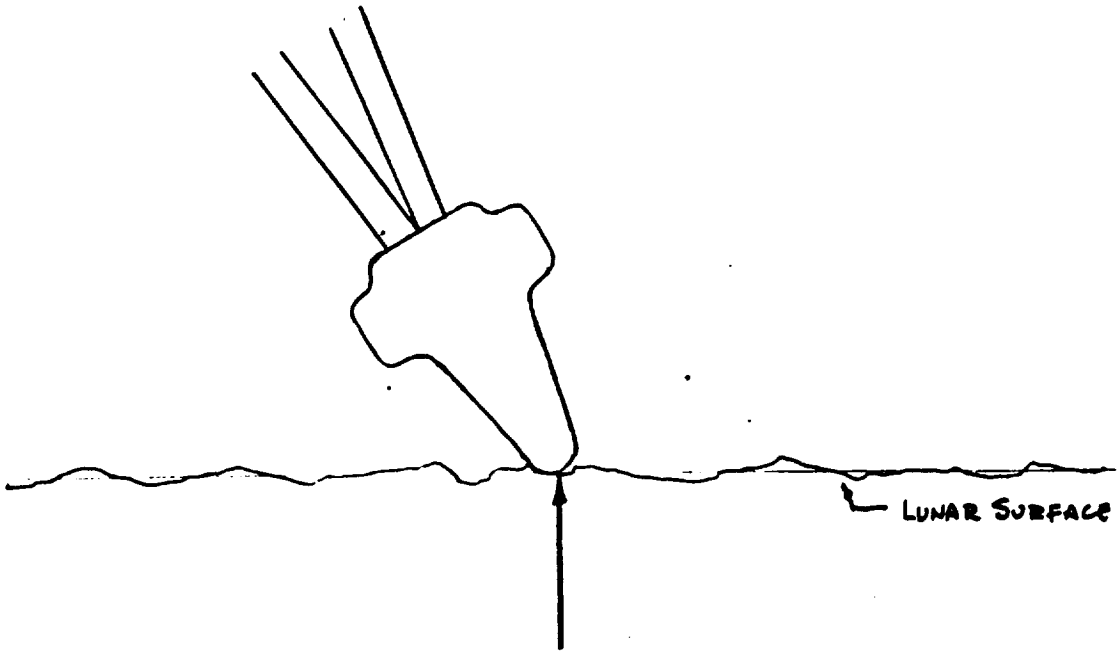

FORCE FROM CRANE OPERATION

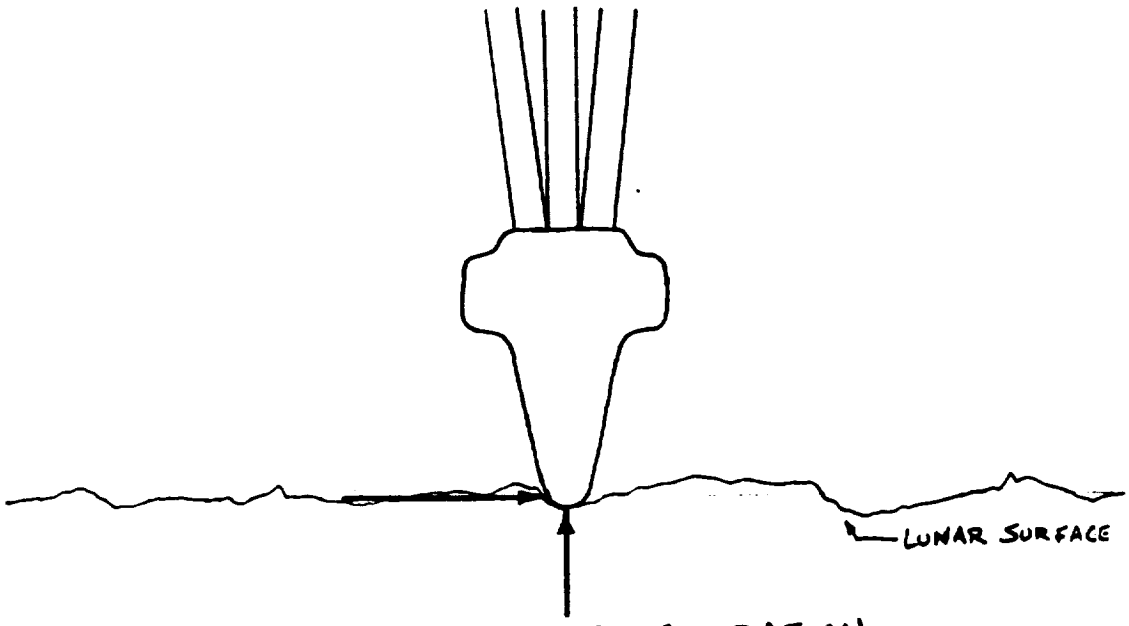

ASSUMED FORCE CONFIGURATION
FOR DRILLING OPERATION

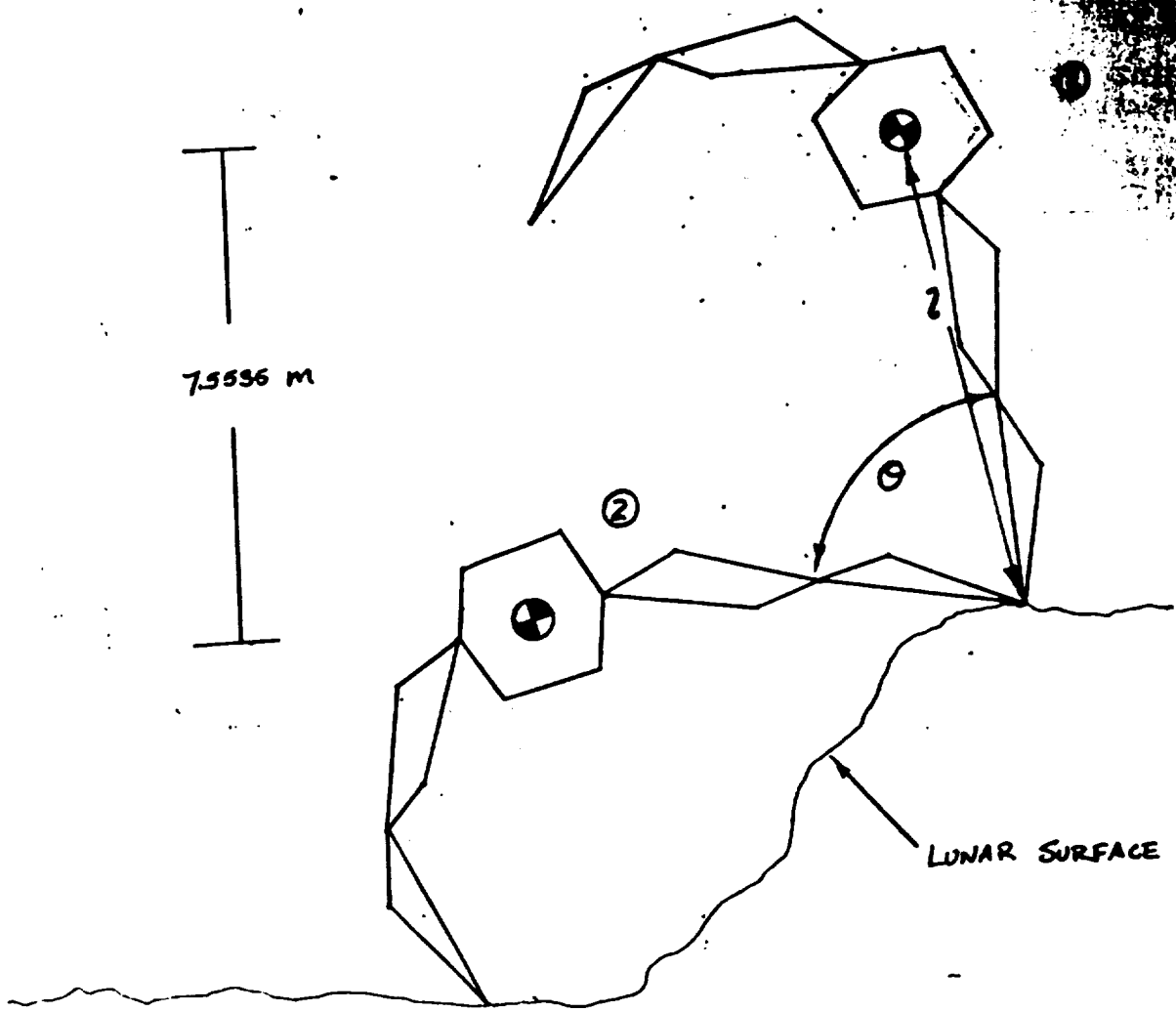

SKITTER MASS

$$12{,}000\ lb_f \left(\frac{1}{32.2\ ft/s^2}\right)\left[\frac{14.6\ kg}{1\ slug}\right] = 5{,}441\ kg$$

ENERGY BALANCE

$$PE_1 + KE_1 = PE_2 + KE_2 = \text{CONSTANT}$$

$$\therefore\ mgh_1 + \tfrac{1}{2}m(\dot{\theta}_1)^2 = mgh_2 + \tfrac{1}{2}m(\dot{\theta}_2)^2$$

$$V_2 = \dot{\theta}_2 = \sqrt{2gh_1} = \sqrt{2\left[\tfrac{1}{6}(9.8\tfrac{m}{s^2})\,7.5535\,m\right]} = 4.97\ \tfrac{m}{s}$$

$\therefore$ FRONT LEG OF SKITTER ENTERS SOIL @ 4.97 m/s

Δ MOMENTUM THROUGH SOIL $= m\Delta V = 5441\ kg\,(4.97-0)\ m/s$

$= 27{,}027\ kg\cdot m/s$

FOR FRONT FOOT TO SUPPORT $\frac{1}{3}$ (Skitter Mass), Δ HEIGHT OF CENTER OF MASS = 1.5 m

$\frac{1}{3}(5541\ kg) = 1847\ kg$

$V_2 = \sqrt{2\left(\frac{1}{6} 9.8 \frac{m}{s^2}\right) 1.5\ m} = 2.2\ m/s$

$m\Delta V = 1847\ kg(2.2\ m/s) = 4089\ kg \cdot m/s$

$\frac{4089\ kg \cdot m/s}{27{,}027\ kg \cdot m/s} = 15.1\%$ of Maximum Δ MOMENTUM

FOR IMPULSE FORCE TO EQUAL CRANE FORCE,

$\frac{m\Delta V}{\Delta t} = \frac{4089\ N \cdot s}{\Delta t} = 31{,}700\ N$

$\therefore \Delta t \geq 0.110$ sec for Impulse Force To Be $\geq$ CRANE FORCE

IMPACT FORCE ANALYSIS

F = (M*DV)/Dt

Mass of Skitter = 27027 kg
Change in vel. = 4.967 m/sec
DMomentum = m*DV = 134243 kg-m/sec

Dtime (sec)	Force (N)
1.000	134243
0.995	134918
0.990	135599
0.985	136287
0.980	136983
0.975	137685
0.970	138395
0.965	139112
0.960	139837
0.955	140569
0.950	141309
0.945	142056
0.940	142812
0.935	143576
0.930	144347
0.925	145128
0.920	145916
0.915	146714
0.910	147520
0.905	148335
0.900	149159
0.895	149992
0.890	150835
0.885	151687
0.880	152549
0.875	153421
0.870	154302
0.865	155194
0.860	156097
0.855	157009
0.850	157933
0.845	158868
0.840	159813
0.835	160770
[illegible]	161739
[illegible]	[illegible]
[illegible]	[illegible]
0.815	[illegible]
0.810	165732
0.805	166762
0.800	167804

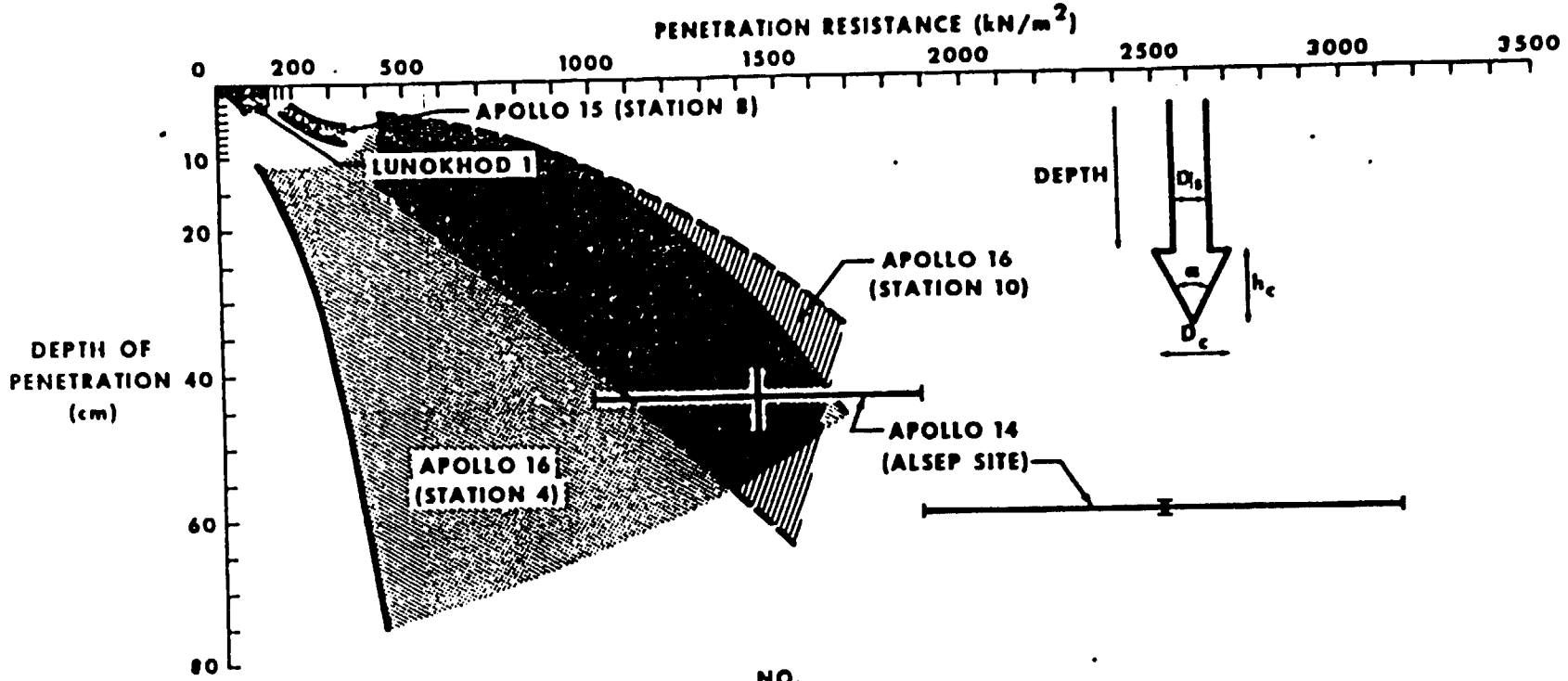

MISSION	NO. OF TESTS	D_c (cm)	α	h_c (cm)	D_s (cm)
APOLLO 14	3	0.95	30°	1.78	0.95
LUNOKHOD 1	327	5.0	60°	4.4	–
APOLLO 15	2	2.03	30°	3.78	0.94
APOLLO 16 (STATION 4)	1	2.03	30°	3.78	0.94
	3	1.28	30°	2.39	0.94
APOLLO 16 (STATION 10)	1	2.03	30°	3.78	0.94
	3	1.28	30°	2.39	0.94

FIG. 3-8 PENETRATION RESISTANCE OF THE LUNAR SURFACE AT DIFFERENT LOCATIONS

APPENDIX 7-2

Cone Point Radius (cm)	Desired Depth (cm)	Static Force (kN)	Max. Pen. Res. (kN/m2)	Avg. Pen. Res. (kN/m2)	Min. Pen. Res. (kN/m2)	Max. Req. Area (cm2)	Avg. Req. Area (cm2)	Min. Req. Area (cm2)	Max. Radius @ Des. Depth (cm)	Avg. Radius @ Des. Depth (cm)	Min. Radius @ Des. Depth (cm)	Max. Total Cone Angle (deg)	Min. Total Cone Angle (deg)	Avg. Total Cone Angle (deg)	Avg. Cone Radius @base of Ring (cm)
5.000	5	31.7	550	325	100	3170	975.4	576.4	31.77	17.62	13.54	158.84	119.33	136.77	51.48
5.000	10	31.7	900	500	100	3170	634.0	352.2	31.77	14.21	10.59	139.03	53.40	85.26	38.86
5.000	15	31.7	1100	625	150	2113.3	507.2	293.2	25.94	12.71	9.59	108.76	33.94	54.38	37.85
5.000	20	31.7	1300	740	180	1761.1	428.4	243.8	23.68	11.68	8.81	86.08	21.57	35.92	20.83
5.000	25	31.7	1500	850	200	1585.0	372.9	211.3	22.46	10.90	8.20	69.87	14.60	25.54	15.48
5.000	30	31.7	1600	925	250	1268.0	342.7	198.1	20.09	10.44	7.94	53.41	11.20	20.57	13.93
5.000	35	31.7	1700	1000	300	1056.7	317.0	186.5	18.34	10.05	7.70	41.73	8.34	16.40	12.13
5.000	40	31.7	1800	1060	320	990.6	299.1	176.1	17.76	9.76	7.49	35.32	7.12	13.56	10.90

VARIABLES
Cpr = cone point radius
Dep = Desired penetration
For = Maximum force applied
Maxres = Maximum penetration resistance
Minres = Minimum penetration resistance
Avgres = Average penetration resistance
Maxara = Maximum required area
Minara = Minimum required area
Avgara = Average required area
Rmax = Radius at maximum area
Rmin = Radius at minimum area
Ravg = Radius at average area
Amax = Maximum total cone angle
Amin = Minimum total cone angle
Aavg = Average total cone angle

CALCULATIONS
Avgres = (Maxres + Minres)/2
Maxara = (For/Minres) * 10000
Minara = (For/Maxres) * 10000
Avgara = (For/Avgres) * 10000
Rmax = (Maxara/3.14159)^0.5
Rmin = (Minara/3.14159)^0.5
Ravg = (Avgara/3.14159)^0.5
Amax = 2*(arctan((Rmax-Cpr)/Dep))
Amin = 2*(arctan((Rmin-Cpr)/Dep))
Aavg = 2*(arctan((Ravg-Cpr)/Dep))

Appendix 7-2A

Sample Calculations

For 20 cm. Penetration: Maxres = 1300 kN/m^2 (From App. 7-1)
Minres = 180 kN/m^2

$$Avgres = (Maxres + Minres)/2$$
$$= \left(\frac{1300 + 180}{2}\right) kN/m^2 = 740\ kN/m^2$$

Area Calculations

(1) $$Maxara = (For/Minres) \times 10{,}000$$
$$= \left(\frac{31.7\ kN}{180\ kN/m^2}\right) \times \frac{10{,}000\ cm^2}{m^2}$$
$$Maxara = 1761.1\ cm^2$$

(2) $$Minara = (For/Maxres) \times 10{,}000$$
$$= \left(\frac{31.7\ kN}{1300\ kN/m^2}\right) \times \left(\frac{10{,}000\ cm^2}{m^2}\right)$$
$$Minara = 243.8\ cm^2$$

(3) $$Avgara = (For/Avgres) \times 10{,}000$$
$$= \left(\frac{31.7\ kN}{740\ kN/m^2}\right) \times \left(\frac{10{,}000\ cm^2}{m^2}\right)$$
$$Avgara = 428.4\ cm^2$$

Radius Calculations

(1) $$Rmax = (Maxara/\pi)^{1/2}$$
$$= \left(\frac{1761.1\ cm^2}{\pi}\right)^{1/2}$$
$$Rmax = 23.68\ cm$$

(2) $$Rmin = (Minara/\pi)^{1/2}$$
$$= \left(\frac{243.8\ cm^2}{\pi}\right)^{1/2}$$
$$Rmin = 8.81\ cm$$

(3) $$Ravg = (Avgara/\pi)^{1/2}$$
$$= \left(\frac{428.4\ cm^2}{\pi}\right)^{1/2}$$
$$Ravg = 11.68\ cm$$

Cone Angle Calculations

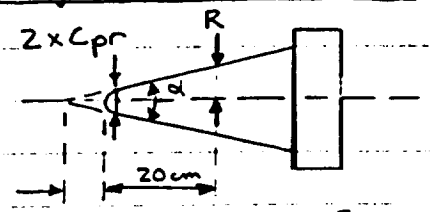

α = cone angle

(1) $A_{max} = 2 \times \arctan\left[\frac{(R_{max} - C_{pr})}{Dep}\right]$

$= 2 \times \arctan\left[\frac{(23.68 - 5)}{20}\right]$

$A_{max} = 86.09°$

(2) $A_{min} = 2 \times \arctan\left[\frac{(R_{min} - C_{pr})}{Dep}\right]$

$= 2 \times \arctan\left[\frac{8.81 - 5}{20}\right]$

$A_{min} = 21.57°$

(3) $A_{avg} = 2 \times \arctan\left[\frac{(R_{ave} - C_{pr})}{Dep}\right]$

$= 2 \times \arctan\left[\frac{11.68 - 5}{20}\right]$

$A_{avg} = 36.94°$

APPENDIX 7-3

CALCULATIONS AFTER CONICAL AREA ADJUSTED FOR CRANE ANGLE (51.56 deg)

Cone Point Radius (cm)	Desired Depth (cm)	Static Force (kN)	Max. Pen. Res. (kN/m2)	Avg. Pen. Res. (kN/m2)	Min. Pen. Res. (kN/m2)	Max. Req. Area @ Des. Depth (cm2)	Avg. Req. Area @ Des. Depth (cm2)	Min. Req. Area @ Des. Depth (cm2)	Adj. Max. Req. Area @ Des. Depth (cm2)	Adj. Avg. Req. Area @ Des. Depth (cm2)	Adj. Min. Req. Area @ Des. Depth (cm2)	Max. Radius @ Des. Depth (cm)	Avg. Radius @ Des. Depth (cm)	Min. Radius @ Des. Depth (cm)	Max. Total Cone Angle (deg.	Min. Total Cone Angle deg)	Avg. Total Cone Angle (deg
5.000	5	31.7	550	325	100	3170.00	975.38	576.36	1970.77	606.39	358.32	25.05	13.89	10.68	151.99	97.89	121.31
5.000	10	31.7	900	500	100	3170.00	634.00	352.22	1970.77	394.15	218.97	25.05	11.20	8.35	126.98	37.03	83.61
5.000	15	31.7	1100	625	150	2113.33	507.20	288.18	1313.85	315.32	179.16	20.45	10.02	7.55	91.69	19.31	37.01
5.000	20	31.7	1300	740	180	1761.11	428.33	243.85	1094.87	266.32	151.60	18.67	9.21	6.95	68.70	11.12	23.75
5.000	25	31.7	1500	850	200	1585.00	372.94	211.33	985.39	231.86	131.38	17.71	8.59	6.47	53.90	6.72	16.35
5.000	30	31.7	1600	925	250	1268.00	342.70	198.13	788.31	213.06	123.17	15.84	8.24	6.26	39.74	4.82	12.31
5.000	35	31.7	1700	1000	300	1056.67	317.00	186.47	656.92	197.08	115.93	14.46	7.92	6.07	30.25	3.52	9.54
5.000	40	31.7	1800	1060	320	990.63	299.06	176.11	615.87	185.92	109.49	14.00	7.69	5.90	25.36	2.59	7.73

VARIABLES

Cpr = cone point radius
Dep = Desired penetration
For = Maximum force applied
Maxres = Maximum penetration resistance
Minres = Minimum penetration resistance
Avgres = Average penetration resistance
Maxara = Maximum required area
Minara = Minimum required area
Avgara = Average required area
Amaxara = Adjusted maximum area
Aminara = Adjusted minimum area
Aavgara = Adjusted average area
Rmax = Radius at maximum area
Rmin = Radius at minimum area
Ravg = Radius at average area
Amax = Maximum total cone angle
Amin = Minimum total cone angle
Aavg = Average total cone angle

CALCULATIONS

Avgres = (Maxres + Minres)/2
Maxara = (For/Minres) * 10000
Minara = (For/Maxres) * 10000
Avgara = (For/Avgres) * 10000
Amaxara = Maxara * Cos(51.56)
Aminara = Minara * Cos(51.56)
Aavgara = Avgara * Cos(51.56)
Rmax = (Amaxara 3.14159
Rmin = Aminara 3.14159
Ravg = Aavgara 3.14159
Amax = Inverse Tangent
Amin = Inverse Tangent
Aavg = Inverse Tangent

Sample Calculations

For 20 cm Penetration: Maxres = 1300 $\frac{kN}{m^2}$ (From App. 7-1)

Minres = 180 $\frac{kN}{m^2}$

Avgres = (Maxres + Minres / 2)

= $\left(\frac{1300 + 180}{2}\right)$ = 740 kN/m^2

For Area calculations, see App. 7-2

Adjusted Area Calculations

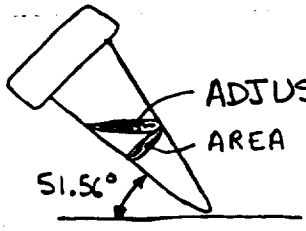

Adjusted Area = Area x cos (51.56)

(1) Amaxara = Maxara x cos 51.56

= 1761.11 x cos 51.56

Amaxara = 1094.87 cm^2

(2) Aminara = Minara x cos (51.56)

= 243.85 x cos (51.56)

= 151.60 cm^2

(3) Aavgara = Avgara x cos (51.56)

= 428.33 x cos (51.56)

= 266.32 cm^2

Radius Calculations

(1) Rmax = $(Amaxara/\pi)^{1/2}$

= $(1094.87/\pi)^{1/2}$

Rmax = 18.67 cm

$R_{min} = (A_{minara}/\pi)^{1/2}$
$= (151.60/\pi)^{1/2}$
$= 6.95$ cm.

$R_{avg} = (A_{avgara}/\pi)^{1/2}$
$= (266.32/\pi)^{1/2}$
$= 9.21$ cm

For Cone Angle calculations, see App. 7-2

Appendix 7-4

Weight Calculations for the Foot

Assumptions: Fillets and rounded corners are not considered. All dimensions in cm.

From Figure 10

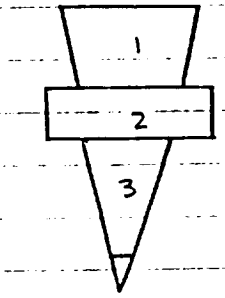

Volume 1

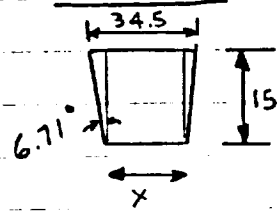

$x = 34.5 - (2)(15)(\tan 6.71°)$

$x = 31$ cm.

$V_1 = \pi r^2 h$

$= \pi \left(\frac{34.5+31}{2}\right)^2 15$

$V_1 = 12,634 \text{ cm}^3$

Volume 2

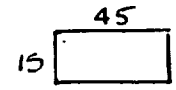

$V_2 = \pi r^2 h$

$= \pi \left(\frac{45}{2}\right)^2 (15)$

$V_2 = 23,856 \text{ cm}^3$

Volume 3

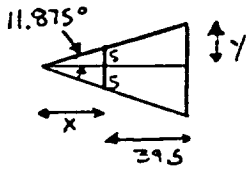

$\tan(11.875°) = \frac{5}{x}$

$x = 23.8$

$x + 39.5 = 63.3$

$\tan(11.875) = \frac{y}{63.3}$

$y = 13.3$

$V_3 = \frac{1}{3}\pi r_1^2 h - \frac{1}{3}\pi r_2^2 h$

$= \frac{1}{3}(\pi)(13.3)^2(63.3) - (\frac{1}{3})(\pi)(5)^2(23.8)$

$V_3 = 11,113 \text{ cm}^3$

Total Volume = $V_{TOT} = V_1 + V_2 + V_3$

$V_{TOT} = 47,607 \text{ cm}^3$

$V_{TOT} = 0.0476 \text{ m}^3$

Weight = $0.0476 \text{ m}^3 \left(\frac{4510 \text{ kg}}{\text{m}^3}\right) = 214.71 \text{ kg}$

Weight $\left(\frac{\text{lb}}{2.2}\right) = \frac{(2)(214.71)}{5454 + 3(214.71)}$

Weight (lb) = 10.6 lb of skin per ft.

Appendix 7-5

Weight Calculations for Final Design

Assumptions: Fillets and rounded corners are not considered. All dimensions in cm.

From Figure 11:

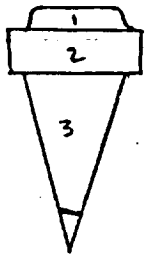

Volume 1

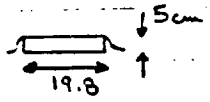

$$V_1 = \pi r^2 h = \pi \left(\frac{19.8}{2}\right)^2 (5)$$

$$V_1 = 1539.5\ cm^3$$

Volume 2

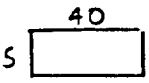

$$V_2 = \pi r^2 h$$

$$= (\pi)(20)^2(5)$$

$$V_2 = 18,849.6\ cm^3$$

Volume 3

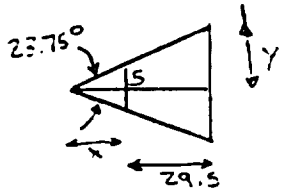

$$\tan(11.875) = \frac{5}{x}$$

$$x = 23.8$$

$$\tan(11.875) = \frac{y}{x + 29.5}$$

$$y = 11.21$$

$$V_3 = \frac{1}{3}\pi r_1^2 h - \frac{1}{3}\pi r_2^2 h$$

$$= \frac{1}{3}\pi (11.21)^2 (23.8 + 29.5) - \frac{1}{3}\pi (5)^2 (23.8)$$

$$V_3 = 6462.3$$

$$V_{TOT} = V_1 + V_2 + V_3$$

$$V_{TOT} = 26,851.4\ cm^3 = 0.0268\ m^3$$

$$Weight = (0.0268 m^3)\left(\frac{4510\ kg}{m^3}\right)$$

$$Wt. = 120.87\ kg$$

$$Wt(\%) = \frac{(3)(120.87)}{5.1 \times 9 + (3)(120.87)}$$

$$\approx 6.23\%$$

FORCE COMPONENTS - CRANE OPERATION

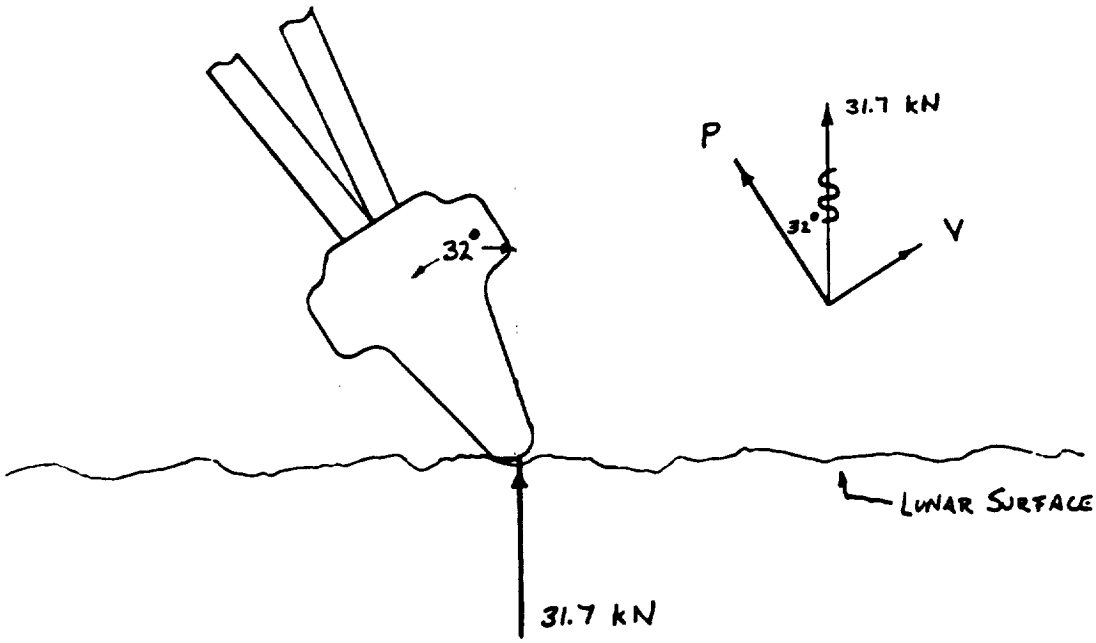

$P = 31.7 \cos(32^\circ) = 27.0 \text{ kN}$

$V = 31.7 \sin(32^\circ) = 16.8 \text{ kN}$

SAMPLE CALCULATIONS

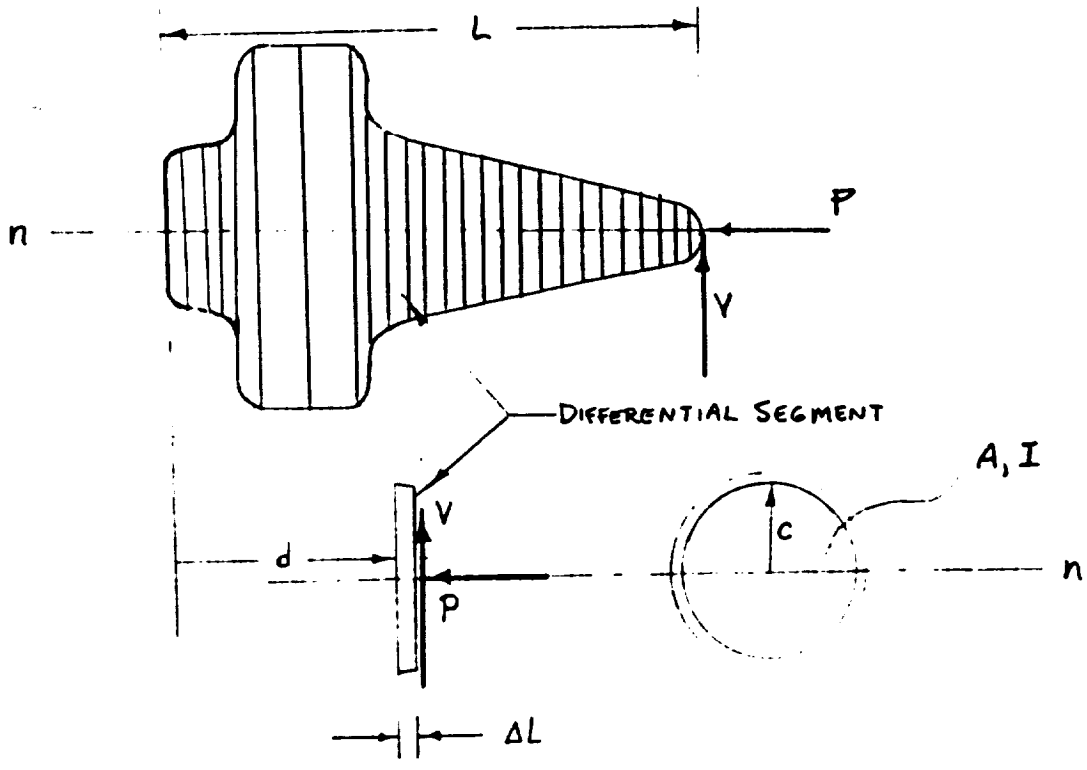

DIMENSIONS

A	Cross-Sectional Area of Differential Segment
c	Radius of Differential Segment (Distance from neutral axis)
d	Length of Foot from Base to Differential Segment
I	Moment of Inertia
ΔL	Differential Length of Segment
n	neutral axis
L	Total Length of Foot (0.545 m)
V	Shear Force (27.0 kN)
P	Normal Force (16.8 kN)

CALCULATIONS

NORMAL STRESS $\sigma = P/A$

BENDING STRESS $\sigma = Mc/I = \frac{V(L-d)c}{I}$

SHEAR STRESS $\tau = V/A$

DIFFERENTIAL CHANGE IN SEGMENT LENGTH $\delta = \text{delta} = \frac{P(\Delta L)}{EA}$

DEFLECTION OF SEGMENT $\Delta y = \frac{V \Delta L^2 [\Delta L - 3(L-d)]}{6 E I}$

SAMPLE CALCULATIONS

Consider Differential Section @ Base of Foot

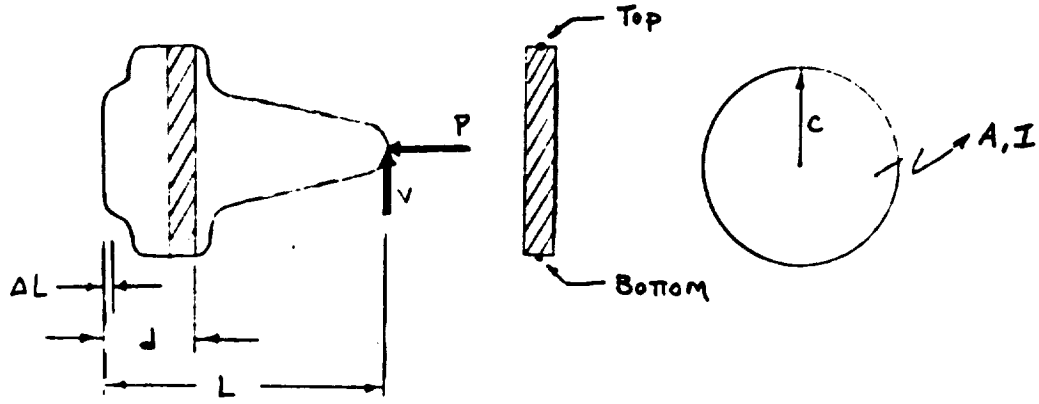

DIMENSIONS

$\Delta L = 0.047$ m (Differential Length)
$L = 0.545$ m (Constant)
$c = 0.200$ m
$d = 0.172$ m (Length of Foot from Base)

$V = 27.0$ kN
$P = -16.8$ kN

AREA $A = \pi c^2 = \pi (0.200)^2 = 0.1256\ m^2$

MOM. OF INERTIA $I = \frac{1}{4}\pi c^4 = \frac{1}{4}\pi (0.200)^4 = 0.00125\ m^4$

BENDING STRESS $\frac{Mc}{I} = \frac{V(L-d)c}{I} = \frac{27.0\ kN\,(0.545-0.172)m\ 0.200m}{0.00125\ m^4} = 1603\ kPa$

NORMAL STRESS $\frac{P}{A} = \frac{-16.8\ kN}{0.1256\ m^2} = -134\ kPa$

SHEAR STRESS $\frac{V}{A} = \frac{-27.0\ kN}{0.1256\ m^2} = -215\ kPa$

NORMAL STRESS SUMMATION

Top $\sigma_T = (-1603 - 134)\ kPa = -1737\ kPa$

Bottom $\sigma_B = (+1603 - 134)\ kPa = 1469\ kPa$

* DEFLECTION OF SEGMENT $y = \frac{V\Delta L^2[\Delta L - 3(L-d)]}{6EI}$

$= \frac{(27{,}000N)(0.047\ m)^2[0.047 - 3(0.545-0.172)]m}{6\,(1.102\times10^{11}\ \frac{N}{m^2})\,0.00125\ m^4}$

$= -7.7\times10^{-8}\ m \approx 0.0\ m$

DIFFERENTIAL CHANGE OF SEGMENT LENGTH $\delta = \frac{P\Delta L}{EA} = \frac{16.800N\,(0.047\ m)}{1.102\times10^{11}\ \frac{N}{m^2}\,(0.1256\ m^2)} = 5.7\times10^{-8}\ m$

$\approx 0.0\ m$

SAMPLE CALCULATIONS

NOTE: SINCE MOMENT OF INERTIA CHANGES OVER LENGTH OF FOOT, DEFLECTION EQN. FROM TABLE A-12-1, P. 804 of SHIGLEY & MITCHELL HAS TO BE MODIFIED AS FOLLOWS:

$$y = \frac{V x^2 (x - 3L)}{6EI}$$

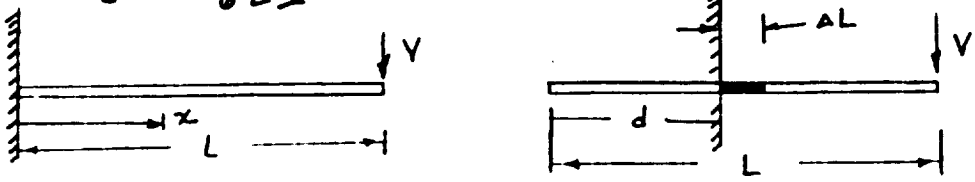

REPLACE: x WITH ΔL

L WITH $(L-d)$

FOR TOTAL DEFLECTION OF FOOT, SUM DEFLECTIONS OF SEGMENTS

NORMAL AND SHEAR STRESS CALCULATIONS -

V = 27000 N
P = 16800 N
Length of Foot = 0.545 m
E = 1E+11 Pa

Radius (m)	Area (m2)	I (m4)	Mc/I (kN/m2)	P/A (kN/m2)	NORMAL STRESS SUMMATION TOP (kN/m2)	NORMAL STRESS SUMMATION BOTTOM (kN/m2)	SHEAR STRESS V/A (kN/m2)	Length of Foot From Base (m)	Defl. (m)	Diff. Length (m)	delta (m)
0.095	0.0282	0.00006	21,922	594	-22515	21,328	954	0.000	0.00000	0.000	0.000000
0.119	0.0444	0.00015	11,036	378	-11414	10,659	607	0.004	-0.00000	0.004	0.000000
0.123	0.0475	0.00017	9,902	353	-10255	9,549	568	0.009	-0.00000	0.005	0.000000
0.129	0.0522	0.00021	8,359	321	-8681	8,038	516	0.023	-0.00000	0.014	0.000000
0.136	0.0581	0.00026	6,943	289	-7232	6,653	465	0.037	-0.00000	0.014	0.000000
0.149	0.0697	0.00038	5,207	241	-5447	4,966	387	0.044	-0.00000	0.007	0.000000
0.176	0.0973	0.00075	3,159	173	-3332	2,987	277	0.044	0.00000	0.000	0.000000
0.197	0.1219	0.00118	2,194	138	-2332	2,057	221	0.057	-0.00000	0.013	0.000000
0.200	0.1256	0.00125	2,041	134	-2175	1,907	215	0.070	-0.00000	0.013	0.000000
0.200	0.1256	0.00125	1,805	134	-1939	1,671	215	0.125	-0.00000	0.055	0.000000
*0.200	0.1256	0.00125	1,603	134	-1737	1,469	215	0.172	-0.00000	0.047	0.000000
0.190	0.1134	0.00102	1,769	148	-1917	1,621	238	0.192	-0.00000	0.020	0.000000
0.176	0.0973	0.00075	2,182	173	-2354	2,009	277	0.199	-0.00000	0.007	0.000000
0.152	0.0725	0.00041	3,387	231	-3618	3,156	372	0.199	0.00000	0.000	0.000000
0.122	0.0467	0.00017	5,418	359	-5777	5,059	577	0.206	-0.00000	0.007	0.000000
0.108	0.0366	0.00010	8,705	458	-9164	8,247	737	0.226	-0.00000	0.020	0.000000
0.102	0.0326	0.00008	9,589	514	-10103	9,075	826	0.249	-0.00000	0.023	0.000000
0.098	0.0301	0.00007	10,008	557	-10565	9,451	895	0.271	-0.00000	0.022	0.000000
0.095	0.0283	0.00006	9,824	593	-10416	9,231	952	0.300	-0.00000	0.029	0.000000
0.088	0.0243	0.00004	11,300	691	-11990	10,609	1,110	0.321	-0.00000	0.021	0.000000
0.081	0.0206	0.00003	12,873	815	-13688	12,058	1,310	0.346	-0.00000	0.025	0.000000
0.075	0.0176	0.00002	13,771	951	-14722	12,821	1,528	0.376	-0.00000	0.030	0.000000
0.068	0.0145	0.00001	15,525	1,156	-16682	14,369	1,859	0.403	-0.00000	0.027	0.000000
0.064	0.0128	0.00001	15,081	1,306	-16387	13,776	2,098	0.430	-0.00000	0.027	0.000000
0.060	0.0113	0.00001	14,165	1,485	-15650	12,679	2,387	0.456	-0.00000	0.026	0.000000
0.054	0.0092	0.00000	14,682	1,820	-16502	12,862	2,926	0.477	-0.00000	0.021	0.000000
0.048	0.0070	0.00000	15,237	2,370	-17607	12,866	3,809	0.498	-0.00000	0.021	0.000000
0.039	0.0048	0.00000	8,439	3,462	-11901	4,976	5,565	0.530	-0.00000	0.033	0.000001
0.027	0.0023	0.00000	13,818	7,282	-21100	6,537	11,702	0.537	-0.00000	0.007	0.000000
									---------		---------
									-0.00000 m		0.0000045 m

CALCULATIONS:

Area	3.1415*(A14^2)
Moment of Inertia	3.1415*(A14^4)/4
Mc/I	+$C$4*($C$6-I14)*A14/(C14*1000)
P/A	+$C$5/(B14*1000)
Normal Stress Summation Top	-E14-F14
Normal Stress Summation Bottom	+E14-F14
Shear Stress	+$C$6/(B14*1000)
Length of Foot to Tip	+$C$6-D14
Deflection	+$C$4*(K14^2)*(K14-(3*($C$6-I14)))/(6*$C$7*C14)
Differential Length	+I15-I14
delta (change in foot length)	+$C$5*L14/($C$7*B14)

* SAMPLE CALCULATION VALUES

(81)

POINTS OF MEASUREMENT - FOOT DESIGN

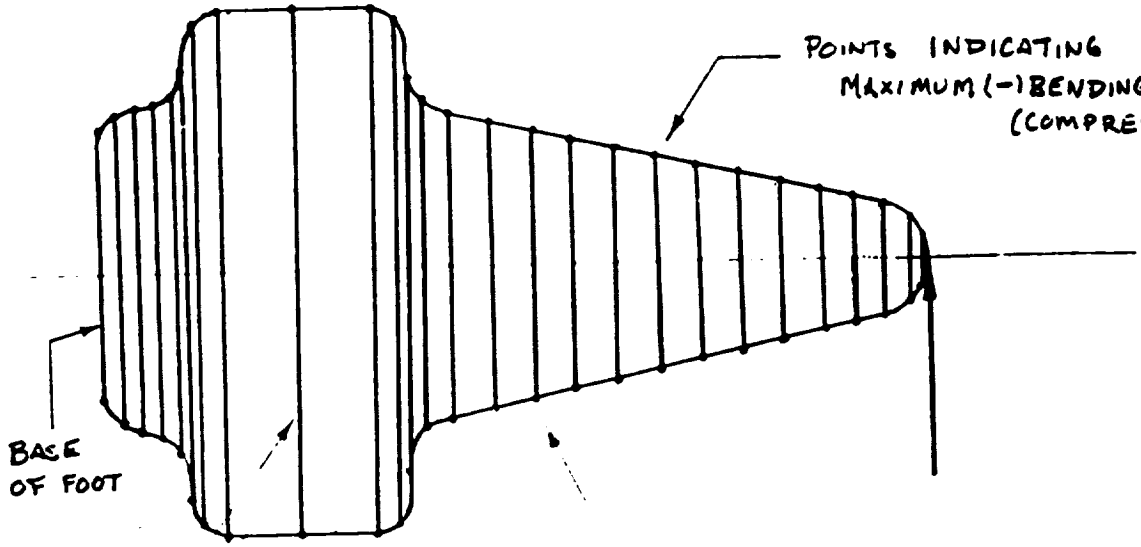

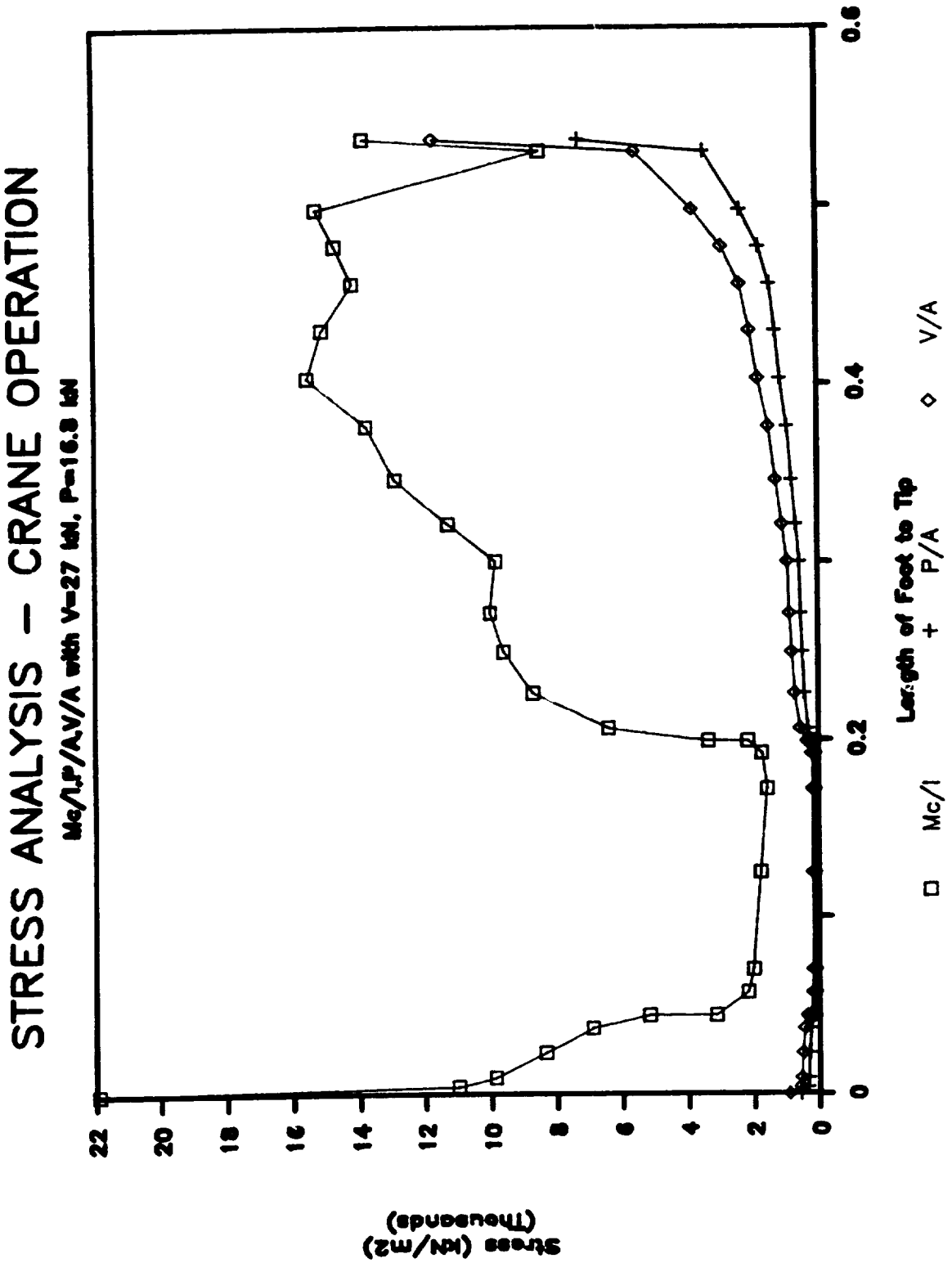
STRESS ANALYSIS – CRANE OPERATION
Mc/I/P/A/V/A with V=27 kN, P=16.8 kN
Stress (kN/m2) (Thousands)
22
20
18
16
14
12
10
8
6
4
2
0
0
0.2
0.4
0.6
Length of Foot to Tip
Mc/I
P/A
V/A

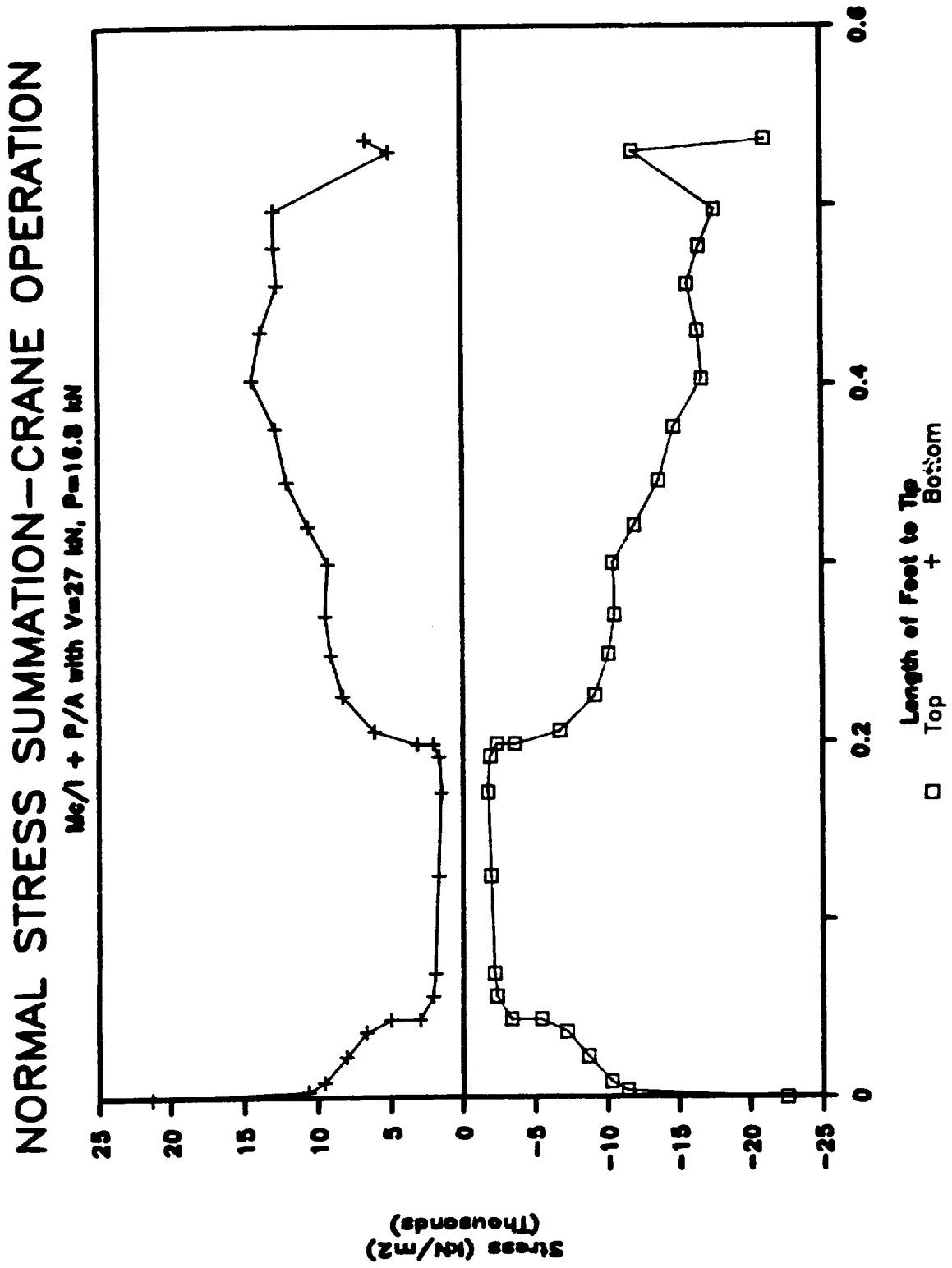
NORMAL STRESS SUMMATION—CRANE OPERATION
Mc/I + P/A with V=27 kN, P=16.8 kN
25
20
15
10
5
0
-5
-10
-15
-20
-25
0
0.2
0.4
0.6
Length of Feet to Tip
Top
Bottom
Stress (kN/m2)
(Thousands)

CANTILEVER CALCULATIONS

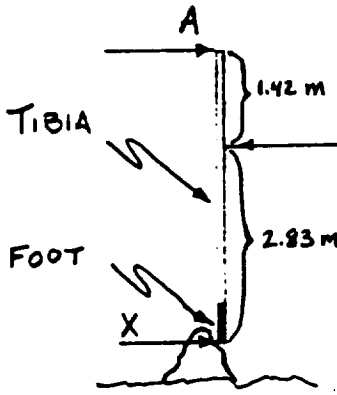

FORCES:

A - FORCE FROM FEMUR

X - FORCE FROM OBJECT IN PATH OF FOOT

$\circlearrowleft A$: $(1.42\ m)\ 138{,}000\ N = (1.42 + 2.83)_m\ X$

$\therefore X = 46{,}100\ N$

$A = 138{,}000 - 46{,}100 = 91{,}900$

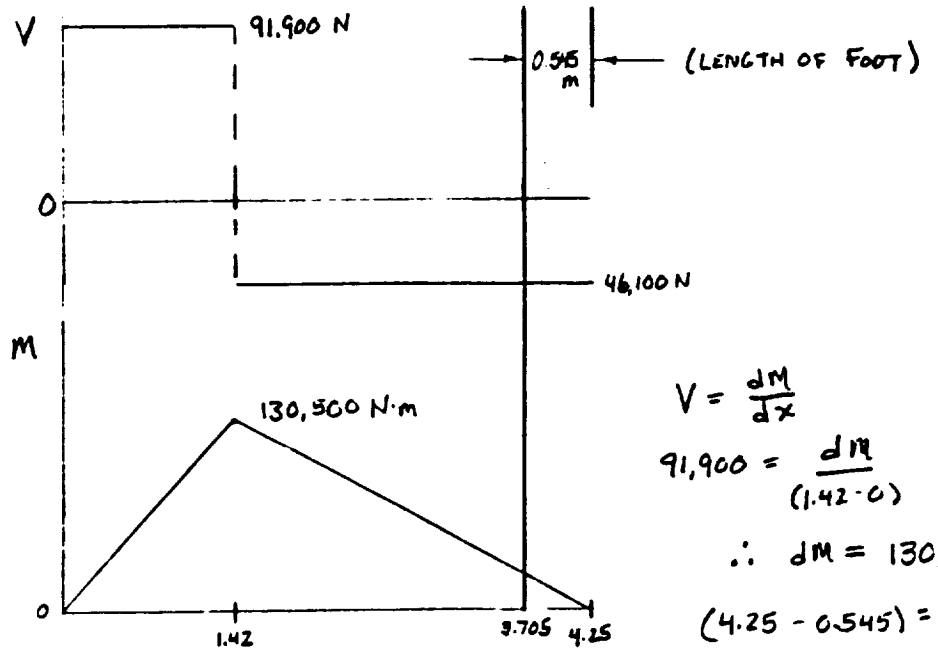

$V = \frac{dM}{dx}$

$91{,}900 = \frac{dM}{(1.42 - 0)}$

$\therefore dM = 130{,}500\ N \cdot m$

$(4.25 - 0.545) = 3.705\ m$

MAXIMUM MOMENT ON FOOT @ BASE ($x = 3.705\ m$)

$\frac{130{,}500}{(4.25 - 1.42)} = \frac{M}{(4.25 - 3.705)}$ $\qquad M = 26{,}100\ N\ m$

$V = 46{,}100\ N$

$M_{max} = 26{,}100\ N \cdot m$

CANTILEVER CALCULATIONS

V = 46100 N
M = 25100 N-m (Top of Foot)
Length of Foot = 0.545 m
E = 1.1E+11 Pa

Radius (m)	Area (m2)	I (m4)	Distance from Top of Foot (m)	Mc/I (kN/m2)	V/A (kN/m2)	Diff. Length (m)	Defl. (m)
0.095	0.028293	0.000064	0.000	37429	1629	0.000	0.00000
0.119	0.044488	0.000157	0.004	18844	1036	0.004	0.00000
0.123	0.047529	0.000180	0.009	16907	970	0.005	0.00000
0.129	0.052279	0.000217	0.023	14273	882	0.014	0.00000
0.136	0.058106	0.000269	0.037	11854	793	0.014	0.00000
0.149	0.069746	0.000387	0.044	8890	661	0.007	0.00000
0.176	0.097313	0.000754	0.044	5394	474	0.000	0.00000
0.197	0.121921	0.001183	0.057	3747	378	0.013	0.00000
0.200	0.125663	0.001257	0.070	3485	367	0.013	0.00000
0.200	0.125663	0.001257	0.125	3082	367	0.055	0.00000
0.200	0.125663	0.001257	0.172	2737	367	0.047	0.00000
0.190	0.113411	0.001024	0.192	3021	406	0.020	0.00000
0.176	0.097313	0.000754	0.199	3725	474	0.007	0.00000
0.152	0.072583	0.000419	0.199	5783	635	0.000	0.00000
0.122	0.046759	0.000174	0.206	10958	986	0.007	0.00000
0.108	0.036643	0.000107	0.226	14864	1258	0.020	0.00000
0.102	0.032685	0.000085	0.249	16372	1410	0.023	0.00000
0.098	0.030171	0.000072	0.271	17088	1528	0.022	0.00000
0.095	0.028352	0.000064	0.300	16773	1626	0.029	0.00000
0.086	0.024328	0.000047	0.321	19294	1895	0.021	0.00000
0.081	0.020611	0.000034	0.346	21979	2237	0.025	0.00000
0.075	0.017671	0.000025	0.376	23513	2609	0.030	0.00000
0.068	0.014526	0.000017	0.403	26508	3173	0.027	0.00000
0.064	0.012867	0.000013	0.430	25750	3583	0.027	0.00000
0.060	0.011309	0.000010	0.456	24185	4076	0.026	0.00000
0.054	0.009228	0.000007	0.477	25068	4995	0.021	0.00000
0.048	0.007088	0.000004	0.498	26015	6504	0.021	0.00000
0.039	0.004852	0.000002	0.530	14409	9501	0.033	0.00000
0.027	0.002307	0.000000	0.537	23594	19991	0.007	0.00000
							-0.00001 m

CALCULATIONS:

Area	3.14159*(A14^2)
Moment of Inertia	3.14159*(A14^4)/4
Mc/I	+$C$3*($C$5-D14)*A14/(C14*1000)
V/A	+$C$3/(B14*1000)
Differential Length	+D15-D14
Deflection	+$C$3*(G14^2)*(G14-(3*($C$5-D14)))/(6*$C$6*C14)

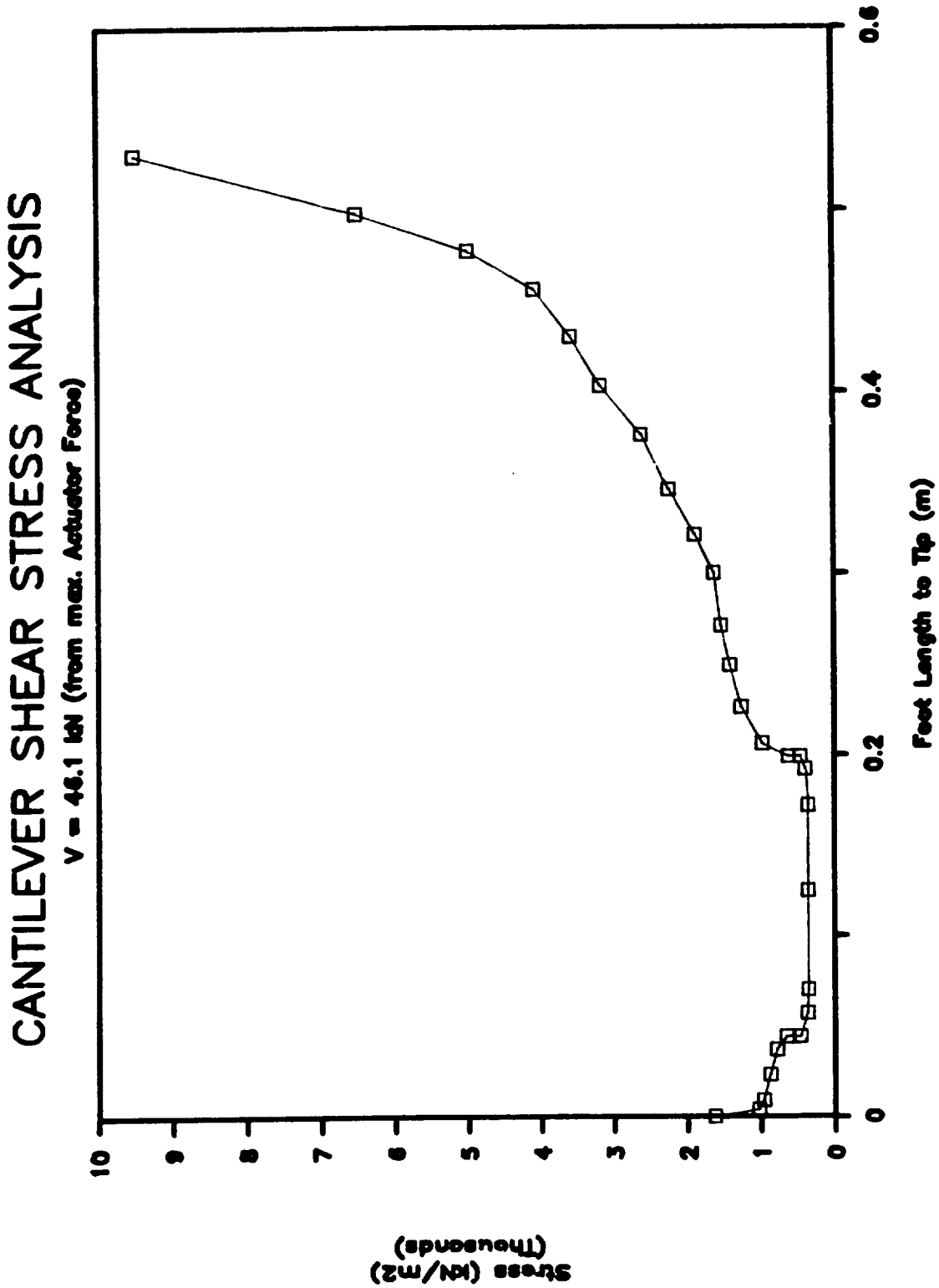
CANTILEVER SHEAR STRESS ANALYSIS
V = 46.1 kN (from max. Actuator Force)
Stress (kN/m2)
(Thousands)
10
9
8
7
6
5
4
3
2
1
0
0
0.2
0.4
0.6
Feet Length to Tip (m)

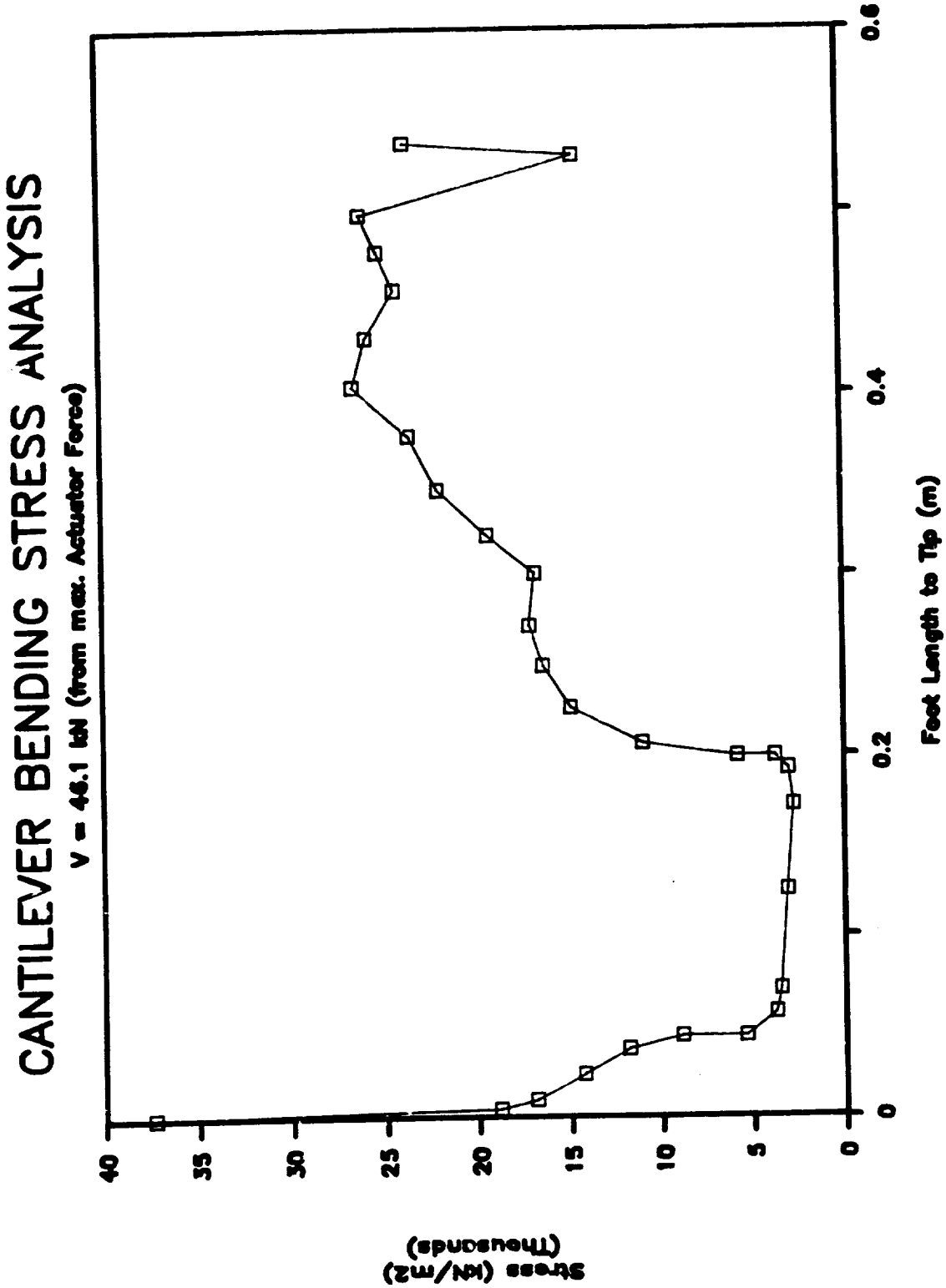
CANTILEVER BENDING STRESS ANALYSIS
V = 46.1 kN (from max. Actuator Force)
Stress (kN/m2)
(Thousands)
40
35
30
25
20
15
10
5
0
0
0.2
0.4
0.6
Foot Length to Tip (m)

CONTINUED

SKITTER FOOT DESIGN
PROGRESS REPORT ONE
GROUP ONE
06-29-87

During the past week our group decided on three initial areas to investigate: lunar environment, material properties, and specifications for the SKITTER. David Jones and Gene Choi investigated the lunar environment. James Morris and Gregg Yancey looked into the specifications for the SKITTER. Martin Parham and Jim Stephens researched the area of material constraints that must be followed.

The purpose of these investigations were to familiarize the group with project background and demands. We are currently working on a problem statement and name for the project.

SKITTER FOOT DESIGN
PROGRESS REPORT TWO
GROUP ONE
07-07-87

DURING THE FIRST WEEK, A PRELIMINARY PROBLEM STATEMENT WAS PREPARED FOR REVIEW. GENE CHOI AND DAVID JONES COMPLETED RESEARCH ON THE LUNAR ENVIRONMENT. THE AREAS RESEARCHED INCLUDED TEMPERATURE VARIATIONS, SOIL CHARACTERISTICS, DUST CONTAMINATION, AND LUNAR GRAVITY CONDITIONS. JAMES MORRIS AND GREGG YANCEY COMPLETED PRELIMINARY RESEARCH ON THE DESIGN SPECIFICATIONS FOR THE SKITTER. THEY HAVE COLLECTED THE NECESSARY REPORTS CONTAINING APPLICABLE DIMENSIONS, WEIGHT, FORCE, AND VELOCITY SPECIFICATIONS FOR THE SKITTER. MARTIN PARHAM AND JIM STEPHENS RESEARCHED THE AREA OF MATERIALS, AND HAVE DETERMINED POSSIBLE CHOICES OF MATERIALS FOR THE FOOT, BASED ON THE ENVIRONMENTAL CONSTRAINTS.

DURING THE CURRENT WEEK, THE GROUP IS USING THE PRELIMINARY RESEARCH TO BEGIN THE DESIGN PROCESS FOR THE FOOT. GREGG YANCEY IS PREPARING A ROUGH DRAFT OF THE FOOT ON THE CADAM SYSTEM. JAMES MORRIS, MARTIN PARHAM, AND JIM STEPHENS ARE CONTINUING THE DISPLACEMENT,FORCE, AND VELOCITY ANALYSIS USING EXISTING SKITTER DATA. THEY ARE COMPILING THE DATA IN SPREADSHEET FORM USING LOTUS SOFTWARE. GENE CHOI IS CONTINUING RESEARCH ON THE FOOT DESIGNS FOR PREVIOUS LUNAR CRAFT. DAVID JONES IS PREPARING THE FINAL EDITION OF THE PROBLEM STATEMENT FOR SUBMISSION. GENE AND DAVID ARE ALSO RESEARCHING THE ASME REQUIREMENTS FOR TECHNICAL REPORTS AND ORAL PRESENTATIONS.

THE GROUP IS EXPECTING TO COMPLETE THE FORCE AND VELOCITY ANALYSIS NEXT WEEK. COMPLETION OF THIS ANALYSIS WILL ALLOW THE GROUP TO BEGIN THE STRESS DETERMINATION AND MATERIAL SELECTION FOR THE SKI POLE DESIGN.

SKITTER FOOT DESIGN
PROGRESS REPORT THREE
GROUP ONE
07-14-1987

During the past three weeks, our group has investigated many areas in the design of the foot for the SKITTER. The group has concluded the research on the lunar environment, and has determined usable materials based on the environment. The group has researched previous lunar missions in order to determine possible foot designs and soil sinkage characteristics for the lunar surface. An initial ski-pole design was prepared as a baseline model.

Martin Parham and Jim Stephens are currently analyzing displacement, force, and velocity data for the SKITTER foot. They have researched the available data and are compiling force and velocity data over the range of motion of the foot. Gregg Yancey and James Morris are using the force data to determine possible modifications to the initial ski pole design. Gene Choi is researching the possible material choices to determine strength and fatigue properties for the applicable materials. David Jones is researching the ASME requirements for the oral presentation and the technical report, as well as preparing the weekly progress report.

The foot design group is planning to use the force analysis data to determine modifications to the initial ski pole design. The group is working toward making a material selection very soon, enabling the force data to be incorporated into the stress analysis of the foot design. Also, an outline of the final design report is to be prepared for the mid-term presentation.

SKITTER FOOT DESIGN
PROGRESS REPORT FOUR
GROUP ONE
07-21-87

THE FOOT DESIGN GROUP IS CURRENTLY CONCENTRATING ON TWO BASIC AREAS WITH OUR DESIGN PROJECT. THE SUBJECTS UNDER STUDY INCLUDE MATERIAL SELECTION AND THE DESIGN CONFIGURATON.

THE CHOICES OF MATERIAL FOR THE SKITTER FOOT HAVE BEEN NARROWED DOWN TO A FEW SELECT MATERIALS. WE ARE CURRENTLY COMPILING THE DATA ON THE DIFFERENT MATERIALS FOR COMPARISION. THE MATERIALS WE ARE CONSIDERING INCLUDE TITANIUM ALLOYS, STAINLESS STEEL ALLOYS, AND COMPOSITES.

THE DESIGN OF THE FOOT HAS BEEN CONSTRAINED TO BE OF THE SKI POLE TYPE. WITH THIS CONSTRAINT, THE GROUP HAS DETERMINED THREE BASIC DESIGNS, WITH POSSIBLE MODIFICATIONS FOR EACH DESIGN. FOR THE MOST PART, THE MODIFICATIONS INVOLVE THE BRACING OF THE RING, AND WILL DEPEND ON THE PROPERTIES OF THE MATERIAL SELECTED.

A PRELIMINARY OUTLINE OF THE FINAL REPORT HAS BEEN PREPARED BY THE GROUP. THE GROUP WILL BE MODIFYING THIS OUTLINE IN PREPARATION FOR THE MID-TERM PRESENTATION. EACH MEMBER IS ASSISTING IN THE PREPARATION FOR THE PRESENTATION, ESPECIALLY IN THE AREAS THE MEMBER HAS RESEARCHED.

SKITTER FOOT DESIGN
PROGRESS REPORT FIVE
GROUP ONE
07-28-87

The foot design group has made much progress in the last week. Decisions have been made in two vital areas, material selection and foot configuration.

Gene Choi and Martin Parham have compiled a list of possible material choices for the foot. Upon analyzing the properties of the different materials, we decided to use ASTM B265-58 T-5 Titanium alloy for the foot.

Jim Stephens and Martin Parham have collected more sinkage data from the Surveyor III mission. After analyzing the sinkage data with our known loads, it was determined that the SKITTER loading was out of range of the data. Extrapolations were made to approximate sinkage. Jim and Martin are researching later missions to find more appropriate sinkage data.

Gregg Yancey has worked extensively on the CADAM system, preparing drawings of all possible designs. Gregg has also prepared drawings for the mid-term presentation.

David Jones and James Morris have worked on the research outline and the mid-term presentation. David prepared the outline, and James assisted in modifying the outline to use in the presentation. James will be making the mid-term presentation. David and Gene prepared this report.

The foo design group has worked very hard to reach the current state. The group is very pleased with the material and design selected. With these decisions behind us, we will begin a detailed analysis of our chosen design, with design modifications performed as necessary.

SKITTER FOOT DESIGN
PROGRESS REPORT SIX
GROUP ONE
08-04-87

The foot design group is now concentrating on finalizing the modified annulus design. Since the group has selected a design as well as a material, we will now be able to dimension our design and analyze it more thoroughly.

Gregg Yancey and James Morris are working to determine the impact forces generated by the SKITTER when it is in walking mode. Knowledge of the impact forces will allow us to determine the sinkage during walking, and the dynamic strength required by the foot.

Jim Stephens is researching coatings for the SKITTER foot. He is currently researching a titanium nitrite coating that would tremendously increase the wear resistance of the foot.

Martin Parham is continuing his research into materials. He has rechecked the material selector program, and reports that there are no weight considerations given. Since the group has already decided to use a space-proven titanium alloy, Martin is compiling all the applicable data on the alloy.

David Jones and Gene Choi are researching the sinkage characteristics of the lunar soil. The Surveyor III sinkage data found earlier was found to be inconclusive for our application, so David and Gene are researching the later missions. Specifically, they are researching the soil experiments from the Appollo 16 mission and relating the data to our application. David and Gene also prepared this report.

SKITTER FOOT DESIGN
PROGRESS REPORT SEVEN
GROUP ONE
08-11-87

The foot design group is now working toward a final design and analysis for the skitter foot. The group is also beginning preparation of the final report.

Martin Parham and Gene Choi are compiling all applicable material data and arranging it in tabular form. They are beginning the preparation of a rough draft of the materials section of the final report, explaining the materials investigation and selection.

Jim Stephens is continuing his research into coatings for the foot. He has collected research data for a titanium nitrate coating and is beginning an analysis of this coating to determine it's effect on the foot.

James Morris is continuing his research into the impact forces generated during the skitter walking motion. These impact forces will be used to determine sinkage during the walking movement.

Gregg Yancey and David Jones are using the latest sinkage data to determine sinkage under known static loads. This analysis is being used to determine the final foot dimensions that will give appropriate sinkage levels during static loads.

David Jones also prepared this report.

SKITTER FOOT DESIGN
PROGRESS REPORT EIGHT
GROUP ONE
08-18-87

The foot design group is currently finishing their work on the SKITTER foot design, and is working to complete the final report. Most of the analysis has been completed, and the design is now finalized.

Martin Parham is preparing the material section of the final report. He is compiling all the researched data and including the data in the report. The materials section of the report will explain the entire course of the materials investigation.

Gene Choi is preparing the environment section of the final report. The environment section of the report will detail all of the environmental conditions relative to the foot design.

Jim Stephens is preparing a section on coating applications for the foot. He is exploring the possibility of a titanium nitride coating for the foot, to reduce wear and corrosion.

Gregg Yancey and James Morris are preparing the final design of the foot. They are examining the weight of the foot in respect to the skitter weight, and altering the design to meet weight goals.

David Jones is preparing the introduction, abstract, and conclusion for the final report. David is also working with Gene Choi in preparing a section on the sinkage analysis for the foot. David Jones prepared this report.

END